Evaluation of the particulate inorganic carbon export efficiency in the global ocean

Jordan Toullec[1]

[1]Univ Brest, CNRS, IRD, Ifremer, UMR 6539, LEMAR, F-29280, Plouzané, France,

Correspondence to: Jordan Toullec (toullec.jordan@gmail.com)

Abstract. The oceanic carbonate pump corresponds to the production and ~~the~~ sinking of particulate inorganic carbon (PIC) ~~thanks to calcified~~by calcifying planktonic organisms. In this study, global estimates of PIC standing stock, production derived from ocean colour, and ~~calcified taxa~~ the contribution of calcifying taxa were combined with PIC flux ~~observation~~observations from short-term sediment traps deployed ~~during~~over the ~~last~~past decades, covering the global ocean. Coccolithophores are the main ~~planktonic calcified~~calcifying plankton group in the euphotic zone, ~~with~~exhibiting a significant seasonal blooming pattern and ~~an important~~a pronounced latitude ~~dependant~~-dependent seasonal response. The present study highlights that ~~the~~ PIC production in the euphotic zone, and the pelagic PIC flux ~~varied~~vary among oceanic regions, ~~depth~~depths, and ~~season~~seasons. Based on a geographic matchup between ~~the~~ PIC flux from sediment traps and remote sensing ~~climatology observation,~~climatological observations, a correlation between net primary production (NPP) of particulate organic carbon (POC) in the euphotic zone and PIC flux is revealed. However, PIC production in the euphotic zone is not correlated with PIC flux at a global scale, but only ~~for delimited~~in specific ocean ~~basin~~basins, such as ~~in~~ the North Atlantic and the Southern Ocean. Despite lower PIC production and PIC/POC ratios in the euphotic zone, temperate and subpolar areas are more efficient ~~to export~~at exporting PIC compared to equatorial and subtropical ~~areas (~~regions, which have higher PIC production and PIC/POC ratios in the euphotic zone~~). The plankton.~~ Plankton phenology ~~seems~~appears to be an important driver of PIC export efficiency (PIC E_{eff}) and PIC transfer efficiency (PIC T_{eff}). This study suggests that the 'packaging factor' ~~corresponding to~~, which includes the ~~vehicle~~vehicles of the biological carbon pump (e.g., marine snow aggregates, fecal pellets) and the plankton network (e.g., zooplankton ~~community~~communities, microbial loop~~) determine the~~), largely determines PIC export ~~efficiency~~ and ~~the PIC~~ transfer ~~efficiency.~~ efficiencies.

1. Introduction

Through gravitational settling, the biological carbon pump (BCP) transports photosynthetically fixed CO_2 into the deep ocean for decades to centuries to come. Without the BCP, atmospheric CO_2 concentration would be twice as high (Passow and Carlson, 2012). Phytoplankton, ~~due to~~through photosynthesis, uptake CO_2 and produce particulate organic carbon (POC). On the other hand, ~~calcified~~calcifying phytoplankton (such as coccolithophores), produce both POC and ~~inorganic carbon (~~particulate inorganic carbon~~, (~~PIC~~);~~). Calcification process, often referred to as calcium carbonate ($CaCO_3$~~), which~~) production, releases CO_2 ~~during the process of calcification~~, this is the

a mis en forme : Police :Arial

a mis en forme : Police :Arial

a mis en forme ...

a mis en forme ...

a mis en forme : Retrait : Gauche : 0 cm, Suspendu : 0,63 cm

a mis en forme : Police :Arial

a mis en forme ...

counter pump effect. Even though calcification contributes to the release of CO_2 (counter effect), all planktonic calcified organisms (such as coccolithophores, foraminifers and pteropods) transport also POC to deep waters through gravitational settling. Field observation of particulate sinking flux (PIC and POC) has been made over many decades to better understand the BCP. To ~~estimate~~measure a particle flux, the sediment traps and Thorium-234 activity (^{234}Th activity) are the most widespread techniques ~~to quantitatively estimate a sinking flux~~, both in terms of time and geography (Savoye et al., 2006, Le Moigne et al., 2014).

Coccolithophores contribute to 70-90% of PIC production in the North Pacific Ocean when nutrient and light are available (Ziveri et al., ~~2023) and~~2023) and more than 90% in the South Atlantic (Kruijt et al., 2026). Coccolithophore are generally considered dominant at global scale (Neukermans et al., 2023). In the global ocean, coccolithophores form mesoscale blooms in high-latitude oceans (Brown and Yoder, 1994; Balch et al., 2005), which are associated with high rates of calcification (Poulton et al., 2007, 2014, Balch et al., 2011; Krumhardt et al., 2017, 2019). The total annual $CaCO_3$ production by planktonic organisms is characterised by a high uncertainty, with a range of 0.7–4.7 Pg C y^{-1} (Berelson et al., 2007; Buitenhuis et al., 2019; Neukermans et al., 2023). A large proportion of these $CaCO_3$ produced in the euphotic zone is dissolved within the first 300m of the ocean (Ziveri et al., 2025, Sulpis et al., 2021, Feely et al., 2002; Milliman et al., 1999~~), thereby increasing ocean alkalinity and CO_2 uptake (Sarmiento, 2013).~~). This shallow dissolution is not yet clearly explained but considered to be associated ~~to~~with biological and ecological mechanisms such as zooplankton and procaryotes mediated dissolution (Sulpis et al., 2021, Kwon et al., 2024, Dean et al., 2024). The sedimentation of calcifying organisms constitutes an export flux of $CaCO_3$ with estimated range of 0.4–1.8 Pg C y^{-1} (Berelson et al., 2007, Neukermans et al., 2023).

At a global scale, particle export efficiency (PE_{eff}, corresponding to the POC sinking flux in the euphotic layer/ POC production) is higher at high latitudes and lower at low latitudes (Henson et al., 2012). ~~The transfer efficiency (T_{eff}, corresponding to the proportion of exported organic matter that reaches the deep ocean), which is lower at high latitudes and higher at low latitudes (Henson et al., 2012). However, satellite estimation of net primary production at low latitude may have large uncertainties, which may result in a bias in the PE_{eff} estimation~~The transfer efficiency (T_{eff}) corresponds to the proportion of exported organic matter that reaches the deep ocean. T_{eff} is lower at high latitudes and higher at low latitudes (Henson et al., 2012)~~, (Henson et al., 2019; Ryan-Keogh et al., 2023; Weber et al., 2016). Recently AI model prediction has been improved and enable the bridge between deep-ocean particles flux observations and satellite images (Picard et al., 2024, 2025). It has been established that T_{eff} is not correlated with $CaCO_3$ export flux (Henson et al., 2012), but evidence from sediment trap collection suggests that coccoliths and coccospheres are transported more efficiently to depth when incorporated into fecal pellets or marine snow aggregates (Honjo, 1976; Pilskaln and Honjo, 1987, Guerreiro et al., 2021, Liu et al., 2022, Toullec et al., 2022). Indeed, the incorporation of biominerals (such as $CaCO_3$ and biogenic silica) induces a ballast effect (excess of density) on marine snow sinking velocity (Iversen and Ploug, 2010; Laurenceau-Cornec et al., 2020) and hence is expected to boost the BCP. However, it has been demonstrated that $CaCO_3$ export flux in the upper ocean is not correlated with the transfer efficiency (Henson et al., 2012), hence the ballast effect hypothesis is still controversial.

Satellite-based estimates of net primary production (NPP) at low latitudes carry substantial uncertainties, potentially biasing PE_{eff} calculations (Henson et al., 2019; Ryan-Keogh et al., 2023; Weber et al., 2016). Recent AI-based models improve the link between deep-ocean particle flux measurements and satellite observations (Picard et al., 2024, 2025). While T_{eff} is not consistently correlated with $CaCO_3$ export flux (Henson et al., 2012), sediment trap

a mis en forme : Police :Arial
a mis en forme : Police :Arial
a mis en forme : Police :Arial
a mis en forme : Police :Arial
a mis en forme : Police :Arial
a mis en forme : Police :Arial
a mis en forme : Police :Arial
a mis en forme : Police :Arial
a mis en forme : Police :Arial, Anglais (Royaume-Uni)
a mis en forme : Police :Arial, Anglais (Royaume-Uni)
a mis en forme : Police :Arial
a mis en forme : Police :Arial
a mis en forme : Police :Arial
a mis en forme : Police :Arial, Anglais (Royaume-Uni)
a mis en forme : Police :Arial, Anglais (Royaume-Uni)

data show that coccoliths and coccospheres are more efficiently transported when incorporated into fecal pellets or marine snow (Honjo, 1976; Pilskaln and Honjo, 1987; Guerreiro et al., 2021; Liu et al., 2022; Toullec et al., 2022). The "ballast effect," postulates that biominerals like $CaCO_3$ and biogenic silica are expected to increase particle density and sinking velocity (Iversen and Ploug, 2010; Laurenceau-Cornec et al., 2020). Hence, BCP is expected to be enhanced by biomineralizing plankton (coccolithophores, diatoms). Nonetheless, the ballast effect remains debated because upper-ocean $CaCO_3$ export flux is not always linked to particle transfer efficiency, leaving the ballast hypothesis controversial (Henson et al., 2012).

Seasonal influence is an important ~~aspect of the~~ factor affecting T_{eff} of carbon to the deep sea ~~and could be attributed to the greater lability of organic matter exported during~~. During phytoplankton blooms~~. In general, high latitudes are opal-productive regions (diatoms blooms) with high PE_{eff} and a higher fraction of~~, the exported organic matter is ~~remineralized before reaching bathypelagic depths (low T_{eff}).~~ more labile, which likely expect to reduce its transfer efficiency. In low latitudes, which are annually ~~$CaCO_3$~~ $CaCO_3$ productive regions, ~~a~~some modelling ~~study~~and observational syntheses have demonstrated that PE_{eff} ~~is~~tends to be lower~~, but~~ while T_{eff} is ~~expected to be~~relatively higher (Henson et al., 2012; Lima et al., 2014~~).~~, Huang & Fassbender, 2024). However, the most recent studies agree that the structure of the ecosystem is a major driver of PE_{eff} and T_{eff}, even more so than latitude (Henson et al., 2019).

The 'packaging factor' theory suggests that $CaCO_3$-dominated ecosystems (subtropics and equatorial area) are associated with a complex food web, and $CaCO_3$ would be more tightly packaged in fast-sinking fecal pellets, associated with potential ballast effect on the POC (Laurenceau-Cornec et al., 2020). However, particle flux from seasonal, opal-dominated systems (Temperate and sub-Polar ecosystems) would be highly "degradable" formed aggregates, produced by the coagulation of senescent diatoms (Francois et al., 2002). This 'packaging factor' as well as the potential associated ballast effect hence should be a strong driver of T_{eff}. Biominerals such as $CaCO_3$ could be a major driver of POC flux (Lacour et al., 2023) or by physically protecting the more labile POC in aggregates from degradation during gravitational settling (Armstrong et al., 2001).

The biogeographical approach is particularly appealing to understand the structures of plankton communities as well as biogeochemical processes according to the latitude and different ocean basins, also under climate change scenarios (Barton et al., 2013). Indeed, biogeographic patterns are common in macroecology (Kaneko et al., 2023; Thuiller et al., 2015), and ~~PCB~~BCP understanding (Clements et al., 2023; Ricour et al., 2023; Wang et al., 2023).

In this context, ocean colour data derived from satellite observation is valuable to estimate surface ocean processes over time. Satellite observations of coccolithophore blooms have been available since the emergence of remote sensing of ocean colour techniques (Holligan et al., 1993). Blooms of coccolithophores (e.g., *Gephyrocapsa (Emiliania) huxleyi*) can ~~result in~~produce highly reflective patches ~~of high reflectivity~~ at the ocean surface ~~of the ocean~~ and ~~are associated with unique~~exhibit distinctive optical properties (Balch et al., 1996, 2005; Balch and Mitchell, 2023~~) that~~). These optical signatures can be used to estimate particulate inorganic carbon (PIC ~~concentration~~) concentrations and production rates at the global scale ~~and production rate~~ (Hopkins & Balch, 2018; Hopkins et al., 2019). There remains a gap in our comprehension of processes controlling the transfer of photosynthetically produced organic carbon to the deep (Buesseler et al., 2007; Henson et al., 2012). Nowadays, heterotrophic respiration in sinking aggregates is considered creating a microenvironment supporting dissolution of $CaCO_3$ in the upper ocean (Morse et al., 2006; Friis et al., 2006; Buitenhuis et al., 2019; Sulpis et al., 2021, Dean et al., 2024). In the deep ocean, dissolution of $CaCO_3$ is primarily driven by conventional thermodynamics of $CaCO_3$ solubility

a mis en forme : Police :Arial

with reduced fluxes of $CaCO_3$ burial to marine sediments. ~~It is estimated~~Kwon et al. (2024) showed that ~~$CaCO_3$~~without $CaCO_3$ dissolution in the upper ocean ~~contribute~~, approximately 20 % more CO_2 would be released to ~~uptake 20% of atmospheric CO_2 through~~ the ~~low latitude upwelling regions (kwon et al., 2024).~~atmosphere.

Understanding how the surface processes control the export of POC and PIC is still an ongoing challenge in the biogeochemical oceanographic community. In addition, processes ~~of~~such as PIC production, sinking flux, and dissolution ~~flux~~ are ~~crucial to understand~~ key components of the ocean alkalinity balance, which ~~control~~in turn regulates atmospheric carbon uptake in surface waters (Renforth ~~&~~and Henderson, 2017; Planchat et al., 2023). This ~~study~~work examines the variability ~~in surface~~of euphotic zone PIC production and deep PIC flux. In this study, a compilation of existing data sources (e.g. PIC flux from sediment traps, calcified taxa group biomass global estimation) and satellite images, geographically covering the open ocean at different seasonal scales is compared and discussed. The objective of this study is to address the following questions: How spatial and seasonal pattern modulate the PIC export efficiency (PIC E_{eff}) and the PIC transfer efficiency (PIC T_{eff}) at the global scale?

2. Materials and Methods

2.1. PIC production remote sensing-based modelling

PIC production at a global scale was modelled using satellite ocean colour measurements (see Hopkins and Balch, 2018 and reference in here for more details), coupled with physiological constant (growth rate under variable light intensity and temperature) associated with *Gephyrocapsa (Emiliania) huxleyi*, which is the most cosmopolitan coccolithophore and extensive blooms former (Holligan et al., 1993) across the majority of the world's oceans (Tyrrell and Merico, 2004).

2.1.1. Calcification model

The model proposed by Hopkins et Balch (2018) was applied to estimate the calcification rate in the euphotic zone (expressed as EZ PIC production). The model of coccolithophores calcification rate is a function of PIC concentration, growth rate, irradiance, and depth (Equation 1):

$$PIC\ production = f[PIC, \mu, h(surf), g(Z_{eu})] \quad (1)$$

In this model, general assumptions are made, such as ~~the~~that PIC production is proportional to the ~~coccolithophore~~coccolithophores growth rate. The ~~coccolithophore~~coccolithophores growth rate is a function of temperature and irradiance (parameters established on *G. huxleyi* culture). The calcification rate decreases as a function of light availability through the water column (Hopkins and Balch, 2018). The model generalizes the euphotic zone integrated PIC production rate (g C m^{-2} d^{-1}) (Equation 2):

$$EZ\ PIC\ production = PIC\ concentration \times \mu \times h\left(I_{surf}\right) \times g(Z_{eu}) \quad (2)$$

Where μ is a temperature-derived growth rate, $h(I_{surf})$ is a growth limiting irradiance function, and $g(Z_{eu})$ is a depth dependency function (see Hopkins and Balch, 2018 and reference inhere for more details). All the satellite products used in the model are described in the following section.

a mis en forme : Police :Arial
a mis en forme : Police :Arial, Non Exposant/ Indice
a mis en forme : Police :Arial
a mis en forme : Police :Arial
a mis en forme : Police :Arial
a mis en forme : Police :Arial
a mis en forme : Police :Arial
a mis en forme : Police :Arial
a mis en forme : Police :Arial
a mis en forme : Police :Arial
a mis en forme : Police :Arial
a mis en forme : Police :Arial
a mis en forme : Police :Arial
a mis en forme : Police :Arial
a mis en forme : Police :Arial
a mis en forme : Police :Arial
a mis en forme : Retrait : Gauche : 0 cm, Suspendu : 0,63 cm
a mis en forme : Retrait : Gauche : 0 cm
a mis en forme : Police :Arial
a mis en forme : Police :Arial
a mis en forme : Police :Arial

2.1.2. PIC and POC standing stock

Surface PIC and POC satellite-based concentrations were depth integrated to ~~100 m to~~100 m using empirical relationships based on *in situ* measurements across the Atlantic Ocean (Balch et al., 2018):

$$PIC_{100m} = 40.555 \times PIC_{surface}{}^{0.560} \quad (3)$$

$$POC_{100m} = 164.376 \times POC_{surface}{}^{0.617} \quad (4)$$

2.1.3. Satellite products collection

The computation was performed with 1° by 1° grid average monthly data (from September 1997 to October 2023) from different sensors merged (Table S1). Satellite ocean color observations are representative the near-surface optical properties (upper 20–40 m in open ocean conditions). The satellite data used in this study (PIC concentration, PAR and Kd_{490nm}) were downloaded from the Globcolour website ~~(https://www.globcolour.info/).~~(https://hermes.acri.fr/, last access: 2 February 2024). The Sea surface temperatures were obtained from NASA Ocean Color website (https://oceancolor.gsfc.nasa.gov/~~)~~, last access: 2 February 2024) and the COPERNICUS marine service website (https://marine.copernicus.eu/fr~~).~~/, last access: 2 February 2024). The following product (Table S1) were used in determining the PIC production rate (g C m^{-2} d^{-1}): ~~The~~the monthly surface PIC concentration (mol C m^{-3}~~); The~~), the monthly SST (Sea Surface Temperature in °C) for the determination of *G. huxleyi* growth rate~~; The~~, the monthly photosynthetic available radiation (PAR; mol photons m^{-2} d^{-1}) for the growth rate limiting irradiance~~; The~~, the monthly Kd_{490nm} (Light diffuse attenuation coefficient at 490 nm; m^{-1}) used for the determination of the euphotic depth and depth-integrated calcification rate, see details of the methods below. Euphotic zone integrated Primary Production (mg C m^{-2} d^{-1}) was obtained from COPERNICUS marine service website (https://marine.copernicus.eu/fr~~/~~, last access: 2 February 2024, DOI:10.48670/moi-00281), the different variables were obtained from multi-sensors products based on SeaWiFS, MERIS, MODIS-A, MODIS-T, VIIRS-SNPP & JPPS1, OLCI-S3A & S3B). The primary production algorithm was developed by Antoine and Morel (1996).

2.1.4. PIC standing stock evaluation, and taxa contribution

Monthly climatology of depth-integrated ~~coccolithophore~~coccolithophores PIC standing stock (g C m^{-2}) in the top 100m was obtained from ocean colour remote sensing using empirical relationships between surface ocean PIC concentration and depth-integrated PIC standing stock (eq. 3, Balch et al., 2018). Monthly climatology PIC standing stock for foraminifers and pteropods in the top 200m was obtained from Knecht et al. (2022; see Fig. 4), supplementary data. The carbon biomass concentration for foraminifers and pteropods in the top 200m (g C m^{-3}) was converted into PIC mass concentration (Bednaršek et al., 2012; Knecht et al., 2023; Schiebel and Movellan, 2012). Integrated PIC standing stock (g C m^{-2}) were obtained for foraminifers and pteropods, by multiplying the PIC biomass concentration (g C m^{-3}) by the layer of integration (200m).

a mis en forme : Retrait : Gauche : 0 cm
a mis en forme : Police :Arial
a mis en forme : Retrait : Gauche : 0 cm
a mis en forme : Police :Arial
a mis en forme : Police :Arial
a mis en forme : Police :Arial
a mis en forme : Police :Arial
a mis en forme : Police :Arial
a mis en forme : Police :Arial
a mis en forme : Police :Arial
a mis en forme : Police :Arial
a mis en forme : Police :Arial
a mis en forme : Police :Arial
a mis en forme : Police :Arial
a mis en forme : Police :Arial
a mis en forme : Retrait : Gauche : 0 cm
a mis en forme : Police :Arial

2.2. PIC flux

PIC productions in the euphotic zone are expressed in g C m^{-2} d^{-1} (as detailed in section 2.1.1). PIC fluxes for the different depth of integration are expressed in g C m^{-2} d^{-1}, considering the deployment duration (in day), the sediment trap collecting surface area (m^2) and the quantity of collected matter (g).

2.2.1. Sediment trap data collection

PIC flux from sediment trap data was obtained from public repositories and published data (https://www.pangaea.de/, see Table S2; Fig. 1).

To ensure that the time scale of the PIC flux corresponds as closely as possible to the products derived from the satellites, analysis on a subset of sediment traps deployed 31 days or less (monthly), for a total of 6057 PIC flux observations (sediment traps deployed from 1983 to 2012) were performed. PIC flux observation was then aggregated into seven different layers of depth (0-100m, 100-500m, 500-1000m, 1000-2000m, 2000-3000m, 3000-4000m and > 4000m), as presented in Table 1. Analysis on monthly deployed sediment flux were matched with monthly remote-sensing climatology (see details in the following section). On the other hand, a possible bias associated with the interaction of hydrodynamics, the capture of zooplankton, organic particle remineralization, and PIC dissolution could happen for a longer time of deployment.

Table 1: Layer of the depth of the subset used in the analysis.

Depth layer	Number of PIC flux observation	Number of sediment traps (location according to 1° by 1° grid map)
0-100m	101	84
100-500m	996	62
500-1000m	1175	54
1000-2000m	1405	64
2000-3000m	730	64
3000-4000m	1077	35
> 4000m	573	28

A total of 262 sediment trap locations were used in the analysis. Note that the total of sediment traps for each layer of depth is equal to ~~388~~391 (multiple sediment traps may have been deployed on the same mooring line), due to the multiple depth ~~deployment~~deployments at the same geographic location. Moreover, multiple PIC flux observations can be attributed to the same sediment trap ~~deployment~~deployments (time series, e.g.: PAP, ALOHA station). As for EZ PIC production model output, the analysis and interpretation of observed PIC flux were applied to the open ocean only, excluding data obtained from a water column of less than 200 m depth.

2.2.2. Global data flux estimates

Total global EZ PIC production (Pg C yr^{-1}) was determined by multiplying integrated PIC production by the latitudinally varying area of each 1° by 1° pixel. The latitude variation pixel surface (m^2) was computed using equation 5:

a mis en forme : Retrait : Gauche : 0 cm, Suspendu : 0,63 cm
a mis en forme : Retrait : Gauche : 0 cm
a mis en forme : Police :Arial
a mis en forme : Police :Arial
a mis en forme le tableau
a mis en forme : Police :Arial
a mis en forme : Police :Arial
a mis en forme : Police :Arial
a mis en forme : Police :Arial
a mis en forme : Police :Arial
a mis en forme : Police :Arial
a mis en forme : Police :Arial
a mis en forme : Police :Arial
a mis en forme : Police :Arial
a mis en forme : Police :Arial
a mis en forme : Police :Arial
a mis en forme : Retrait : Gauche : 0 cm

$$Surface\ (m^2) = \left[\frac{40\,075.017 \times cos\left(\frac{\pi}{180}(Latitude)\right)}{360} \times \frac{\frac{40\,007.864}{2}}{180}\right] \times 10^6 \quad (5)$$

Where the equatorial earth circumference = 40 075.017 km^2 and the meridional earth circumference = 40 007.864 km^2. The data downloaded were a matrix of 180 pixels of latitude by 360 pixels of longitude (based on cylindric projection).

The analysis and interpretation of the EZ PIC production model output were focus on the open ocean only, excluding data obtained from bathymetry lower than 200 m depth.

2.2.3. Biogeochemical regions

RECCAP2 biogeochemical regions (second REgional Carbon Cycle Assessment and Processes) aim to accurately assess land and ocean CO_2 sources and sinks through the efforts of hundreds of scientists around the globe (Hauck et al., 2023). The overall aim of RECCAP2 is to support the Global Carbon Project (https://www.globalcarbonproject.org/) and the stocktaking of greenhouse gases by providing a reliable scientific basis for the transport of carbon between land, ocean and atmosphere. RECCAP2 biogeochemical regions mask was used to aggregate data from sediment traps and remote sensing according to relevant geographical regions (Fig.1, Table S3).

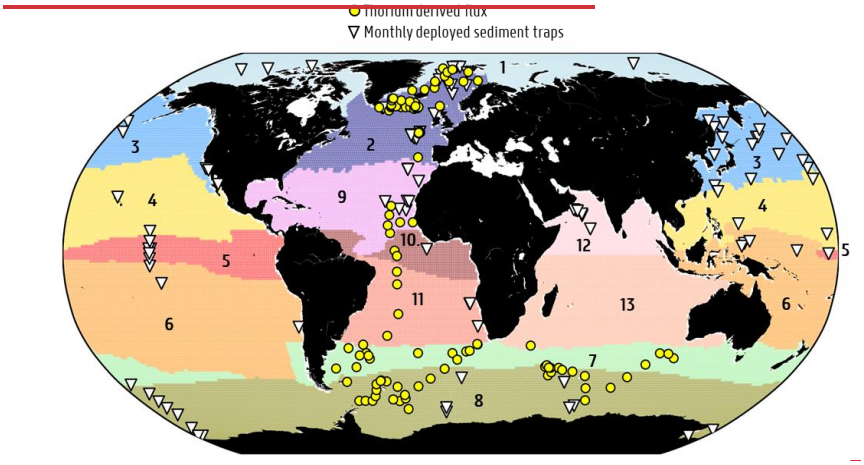

a mis en forme : Police :Arial

a mis en forme : Retrait : Gauche : 0 cm

a mis en forme : Police :Arial

a mis en forme : Police :Arial

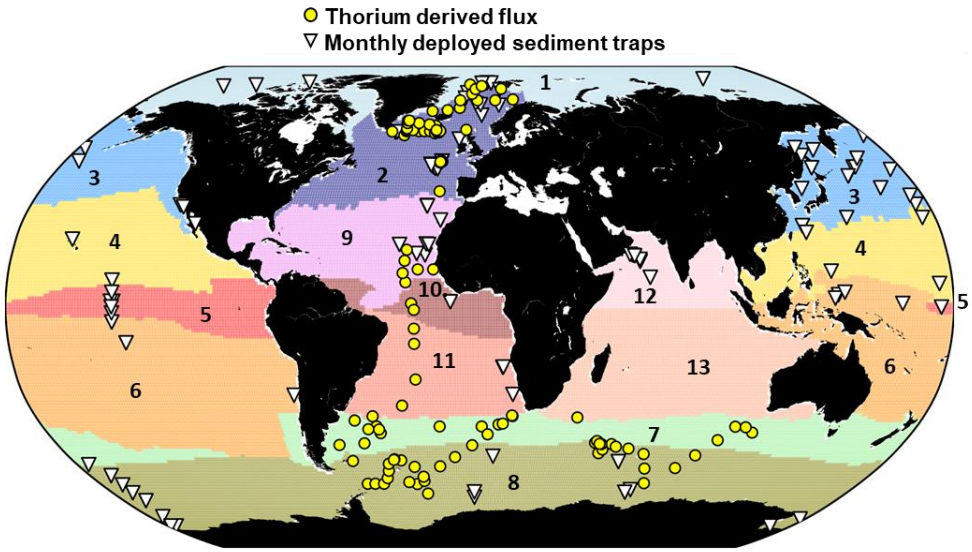

Figure 1: Location of sediment traps measuring PIC flux within 13 biogeochemical regions (RECCAP 2 regions). Region 1 = Arctic (Ar); 2 = North Atlantic (NA); 3 = North Pacific (NP); 4 = North Subtropics Pacific (NSTP); 5 = Equatorial Pacific (EP); 6 = South Subtropics Pacific (SSTP); 7 = Subantarctic (SAZ); 8 = Antarctic (AAZ); 9 = North Subtropics Atlantic (NSTA); 10 = Equatorial Atlantic (EA); 11 = South Subtropics Atlantic (SSTA); 12 = North Indian Ocean (NI) and 13 = South Indian Ocean (SI). The monthly deployed sediment traps are depicted by white triangles and Thorium-derived PIC flux is depicted by yellow dots. 54 stations were out of the RECCAP2 mask (open ocean station) and then have been removed from the 6057 PIC flux observations subset.

a mis en forme : Police :Arial

2.2.4. Euphotic zone integrated satellite-derived production and deep PIC flux matchup

a mis en forme : Retrait : Gauche : 0 cm

The majority of sediment trap ~~deployment~~deployments occurred before the launch of ocean colour observation from satellite, from 1983 to 2012 (SeaWiFS observation started in September 1997). 75.7% of PIC flux data used in the analysis (4588 observations over a total of 6057 observations) were collected before the satellite record. Hence, a match-up between the PIC flux data and EZ PIC production monthly climatology were performed (monthly mean from September 1997 to November 2023).

a mis en forme : Police :Arial

In the analysis, 7 different layers of depth were aggregated (0-100m, 100-500m, 500-1000m, 1000-2000m, 2000-3000m, 3000-4000m and > 4000m). Discrete observed PIC flux values obtained from sediment traps were aggregated over the depth layer of interest and matched geographically with the monthly climatology-modelled EZ PIC production and NPP on the 1°×1° grid. PIC flux values were therefore matched to the same 1° pixel and then associated to the same EZ PIC production. The monthly climatology average of EZ PIC production was established on a period from September 1997 to November 2023 on the 1°×1° grid map. Pearson's correlation test was

performed between the monthly climatology average of EZ PIC production and PIC flux values for the depth layers of interest. The process has been performed for the 13 RECCAP2 biogeochemical regions, covering the global ocean.

EZ PIC production values < 0.1 mg m^{-2} d^{-1} were removed from the dataset, to ~~avoid~~exclude values close to zero or below the detection limit, ~~due to no covering~~which may result from a lack of ~~the~~ satellite coverage. (e.g. winter months in the north hemisphere above 40°N).

2.2.5. Supporting dataset

1° by 1° grid map of fecal ~~pellet~~pellets and aggregates contribution to the total particles export were obtained from model ensemble output from Nowicki et al., 2022 (FigShare database: https://doi.org/10.6084/m9.figshare.19074521).

3. Results

3.1. NPP, PIC production and residence time seasonality

At the global scale, annual EZ PIC production of 1.65 ± 0.36 Pg C y^{-1} was estimated (monthly mean ± σ, 1997-2023 annual mean, 302 months of observation), which is congruent with previous estimation based on the same calcification model (ca. 1.42 ± 1.69 Pg C y^{-1} in Hopkins and Balch, 2018). The difference ~~in~~between the ~~estimation could~~global estimates reported by Hopkins & Balch (2018) and those obtained in this study may be explained ~~by the~~using a merged satellite product ~~quality (resolution) and the number of months used in the model.~~ (see table S1), which provides broader ocean coverage.

The most NPP annual productive areas are located along the continental margins, above 40°N and within equatorial upwelling ecosystems (Fig. 2a). In contrast to the NPP, the most PIC productive areas are located within subtropical gyres, in the Southern Ocean (along the "Great Calcite Belt"), in the North Atlantic, but not in the Northern Indian Ocean, and less productive within equatorial upwelling ecosystems (Fig. 2b). NPP (POC production, Fig 2) is driven by nutrient availability (nitrate, phosphate, iron). Upwelling zones or high-latitude oceans have high nutrient supply, so phytoplankton production is high. Whereases PIC production, especially by *G. huxleyi*, is favoured in nutrient-poor, stable waters (oligotrophic subtropical gyres), where coccolithophores can thrive and calcify efficiently. The seasonal variation of NPP and PIC production follows the phytoplanktonic bloom phenology, with higher seasonal variation above 40°N and below 40°S (Fig. 2c and d). It is noticeable that the PIC production seasonal bias amplitude is higher than NPP seasonal bias (Fig. 2c and d). Both residence time (the integrated stock divided by the integrated production) and amplitude variation are higher for PIC than for POC (Fig. 2e and f). The amplitude of spatial variation of POC residence time is lower than PIC residence time (Fig. 2e and f). The residence time is obtained by dividing the euphotic layer integrated standing stock (g m^{-2}) by the euphotic layer integrated production rate (g m^{-2} d^{-1}). POC residence time highest values reach 20 days in the Southern Ocean and over 20 days in arctic regions (Fig. 2e). However, PIC residence time values reach more than 30 days at high latitudes regions (the Southern Ocean and above 40°C). PIC residence time values over 10 days are also observed within equatorial upwelling (Indian Ocean and West Pacific equatorial). Both PIC and POC residence times reflect a balance between sinking and removal processes such as dissolution or remineralization. For either to sink efficiently,

a mis en forme : Police :Arial
a mis en forme : Police :Arial
a mis en forme : Police :Arial
a mis en forme : Police :Arial
a mis en forme : Police :Arial
a mis en forme : Police :Arial
a mis en forme : Police :Arial
a mis en forme : Police :Arial
a mis en forme : Retrait : Gauche : 0 cm
a mis en forme : Police :Arial
a mis en forme : Police :Arial
a mis en forme : Police :Arial
a mis en forme : Retrait : Gauche : 0 cm, Suspendu : 0,63 cm
a mis en forme : Police :Arial
a mis en forme : Police :Arial
a mis en forme : Police :Arial
a mis en forme : Police :Arial
a mis en forme : Police :Arial
a mis en forme : Police :Arial
a mis en forme : Police :Arial

aggregation into marine snow or incorporation into fecal pellets is generally required. PIC observation (ocean colors based) results mainly from free-floating coccoliths, which can accumulate at the surface to a greater extent than POC. In contrast, POC is readily consumed by bacteria and zooplankton, leading to rapid remineralization in the upper ocean. PIC ($CaCO_3$), however, is chemically more resistant to biological degradation in surface waters and typically dissolves only under specific conditions, such as in undersaturated carbonate waters, in the deep ocean.

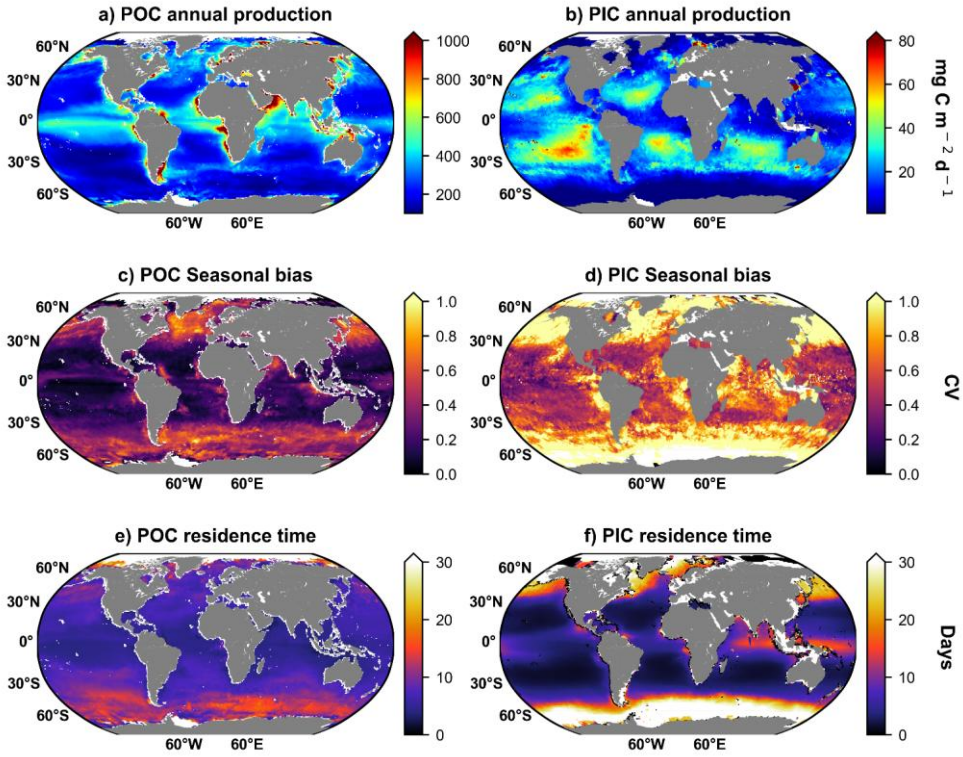

Figure 2: Global maps of (a) POC production (NPP) annual mean (mg ~~POC~~C m^{-2} d^{-1}, 1997-2023 annual mean), (b) PIC production annual mean (mg ~~PIC~~C m^{-2} d^{-1}, 1998-2023 annual mean), (c) NPP seasonal bias expressed as coefficient of variation (σ/μ) of monthly NPP climatology, (c) PIC production seasonal bias expressed as coefficient of variation (σ/μ) of monthly PIC production climatology, (e) POC residence time (day, 1997-2023 annual mean) and (f) PIC residence time (day, 1998-2023 annual mean). POC and PIC residence time is obtained by dividing the annual standing integrated stock (mg m^{-2}) by annual production (mg C m^{-2} d^{-1}), results are expressed in days.

a mis en forme : Police :Arial

a mis en forme : Police :Arial

a mis en forme : Police :Arial

a mis en forme : Police :Arial

a mis en forme : Police :Arial

a mis en forme : Police :Arial

3.2. Taxa contribution to the PIC standing stock estimation

At the global scale, ~~coccolithophore~~coccolithophores PIC standing stock dominates the total estimated PIC standing stock, except in few areas of Equatorial Atlantic (EA), Equatorial Pacific (EP), North Atlantic (NA) and North Pacific (NP), where the pteropods PIC standing stock reach almost 50% (Fig. 3). Foraminifers PIC standing stock represent less than 10% of the PIC standing stock, with higher value in the North Atlantic (NA). Regarding the seasonal variation index, coccolithophores are characterised by high seasonal variation in high latitudes (>30°N and <30°S), while pteropods' seasonal index is higher only >30° N, and in the Equatorial Pacific (EP). Foraminifers tend not to reveal any seasonal variation at a global scale, except in the southeastern North Atlantic (NA) (Fig. 3). Note that the depth of integration is different for coccolithophore (100m) and zooplankton taxa (200m for Pteropods and Foraminifers, from Knecht et al., 2023). Although coccolithophore integration to 100m over 200m for pteropods and foraminifers leads to an underestimation of coccolithophore contribution to the global PIC standing stock in a 200m layer, the general statement that coccolithophore dominates the standing stock remains unchanged. In addition, the foraminifers maximum abundance peak between 0-100m depth (Chaabane et al., 2024).

a mis en forme : Retrait : Gauche : 0 cm, Suspendu : 0,63 cm

a mis en forme : Police :Arial

a mis en forme : Police :Arial

a mis en forme : Police :Arial

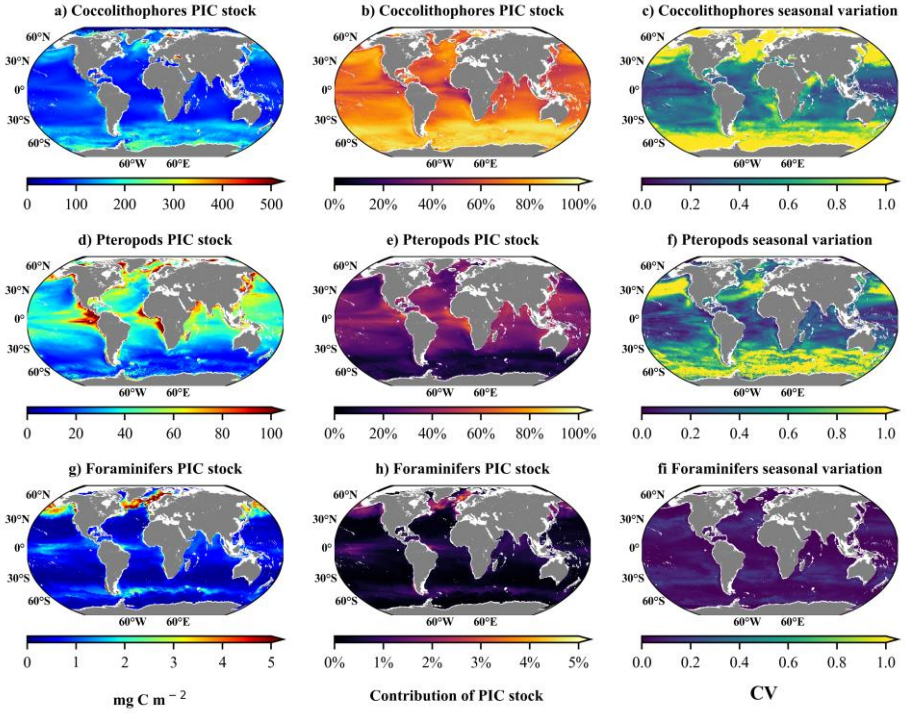

Figure 3: Maps of taxa contribution to the total PIC standing stock regrouping the 3 calcifying taxa: Coccolithophore (a, b and c) Pteropods (d, e and f) and Foraminifers (g, h and i). a, d, and g) Maps of annual PIC standing stock contribution for the 3 calcifying taxa. b, e and h) Maps of annual PIC standing stock for the 3 calcifying taxa. c, f and i) Maps of temporal variability (seasonal index) of PIC standing stock as measured by the seasonal bias (SB) expressed as coefficient of variation (σ/μ) of monthly standing stock for the 3 calcifying taxa. Note that the depth of integration is different for coccolithophore (100m) and zooplankton taxa (200m for Pteropods and Foraminifera, from Knecht et al., 2023).

This study highlights the importance of rapid calcification ~~event observed by satellite (such as blooming~~events. Satellite observations of coccolithophore ~~episodes, monthly), and~~blooms, which typically last less than 30 days ~~integrated~~, suggest that PIC ~~flux~~fluxes from sediment traps ~~(excluding~~should be integrated over short deployments rather than longer ~~deployment).~~periods. Only including short term sediment traps (less than 30 days), give us a picture of relatively fast sedimentation ~~event~~events, this way, coupling with monthly satellite climatology provides greater meaning regarding potential process involved. Despite pteropods and foraminifers contribute to PIC production and deep flux, their seasonality pattern and residence time were not coupled with PIC flux observation, considering short time deployed sediment traps (less than 30 days). In the other hand, other pelagic contributors (Pteropods

a mis en forme : Police :Arial

a mis en forme : Police :Arial

a mis en forme : Police :Arial

a mis en forme : Police :Arial

a mis en forme : Police :Arial

a mis en forme : Police :Arial

a mis en forme : Police :Arial

and foraminifers) are expected to be more peripheral in the export efficiency of the PIC in this study, regarding their respective residence time (more than 30 days for foraminifers and months to year for pteropods). This aspect is the main constraint in the present study. It is assumed that *G. huxleyi* blooms would be present in the water for an average of 30 days (Hopkins et al., 2015), hence, monthly PIC production climatology coverage map represents the mean monthly conditions. Pelagic calcifiers are characterized by different surface stock and seasonality (Fig. 3) and residence time: less than a month for coccolithophore (Hopkins et al., 2015), a month for foraminifers (Schiebel and A. Movellan., 2012) and months to years for pteropods (Lalli & Gilmer.,1989, Bednaršek et al., 2012).

The estimate of calcified taxa PIC stock, including coccolithophores, pteropods, and foraminifera, is not correlated with annual PIC export flux on a global scale (Fig. 4a). These estimates show that coccolithophores dominate the PIC standing stock, followed by pteropods and then foraminifera (Fig. 4). The latitudinal variation in PIC standing stock indicates an overlap between coccolithophore and pteropod PIC standing stock at the equator (Fig. 3b, 3e & Fig. 4b~~), while~~). Coccolithophores and pteropods can contribute roughly equally to the PIC standing stock, but coccolithophores ~~are largely dominant~~dominate at ~~high~~ latitudes ~~(>~~above 40~~°). No correlation between annual PIC standing stock in the surface layer and annual PIC export flux is observed at global scale, regardless of the taxon (Fig. 4a).~~°.

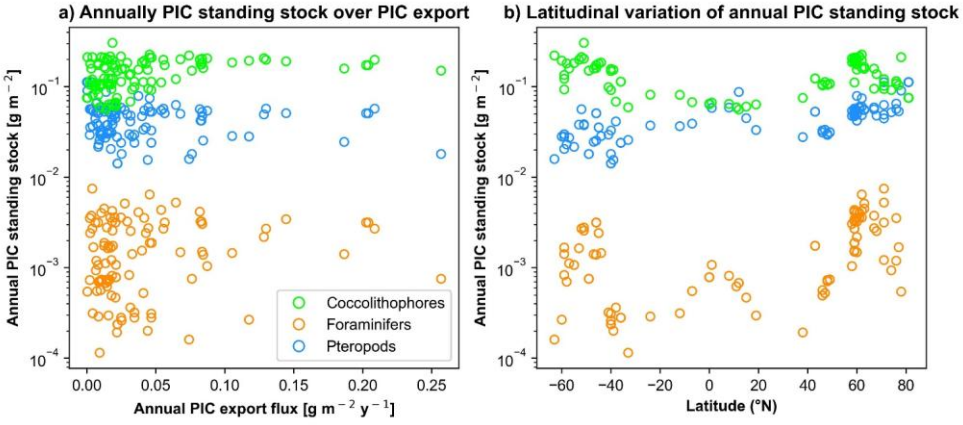

Figure 4: a) Calcifying taxa annual PIC standing stock (g m^{-2}) over annual ^{234}Th-derived PIC flux (g m^{-2} y^{-1}). b) Latitudinal variation of annual PIC standing stock (g m^{-2}) for each calcifying taxa. Only locations where PIC export flux data is shown in this figure. Coccolithophore PIC standing stock is derived from ocean colours (Balch et al., 2005). Pteropods and foraminifers are extracted from Knecht et al. (2023) supplementary data.

a mis en forme : Police :Arial

a mis en forme : Centré, Bordure : Haut: (Pas de bordure), Bas: (Pas de bordure), Gauche: (Pas de bordure), Droite: (Pas de bordure), Entre : (Pas de bordure)

a mis en forme : Police :Arial

a mis en forme : Police :Arial

a mis en forme : Police :Arial

a mis en forme : Police :Arial

a mis en forme : Police :Arial

a mis en forme : Police :Arial

a mis en forme : Police :Arial

3.3. PIC production, NPP and PIC flux

No significant correlation is observed between log-transformed PIC flux and log-transformed NPP ~~is observed between~~ in the ~~surface and 100m depth~~upper 100 m (Fig. 5). On average, ~~despite the~~although Pearson's correlation ~~coefficient R^2 are low (< 0.25), higher R^2~~ coefficients are ~~observed when~~low ($R^2 < 0.25$), the correlation between PIC flux ~~is correlated with~~and NPP ~~compared as compared to~~is generally higher than that between PIC flux and PIC production (Fig. 5). ~~The~~At the deepest layer (>~~4000m) is characterised by higher~~4000 m), however, the correlation between PIC flux and PIC production ~~than~~ ($R^2 = 0.104$) exceeds that between PIC flux and NPP (~~respectively 0.104~~

a mis en forme : Police :Arial
a mis en forme : Retrait : Gauche : 0 cm, Suspendu : 0,63 cm
a mis en forme : Police :Arial
a mis en forme : Police :Arial
a mis en forme : Police :Arial
a mis en forme : Police :Arial
a mis en forme : Police :Arial
a mis en forme : Police :Arial
a mis en forme : Police :Arial
a mis en forme : Police :Arial
a mis en forme : Police :Arial
a mis en forme : Police :Arial
a mis en forme : Police :Arial
a mis en forme : Police :Arial
a mis en forme : Police :Arial

and 0(R^2 = 0.089).)

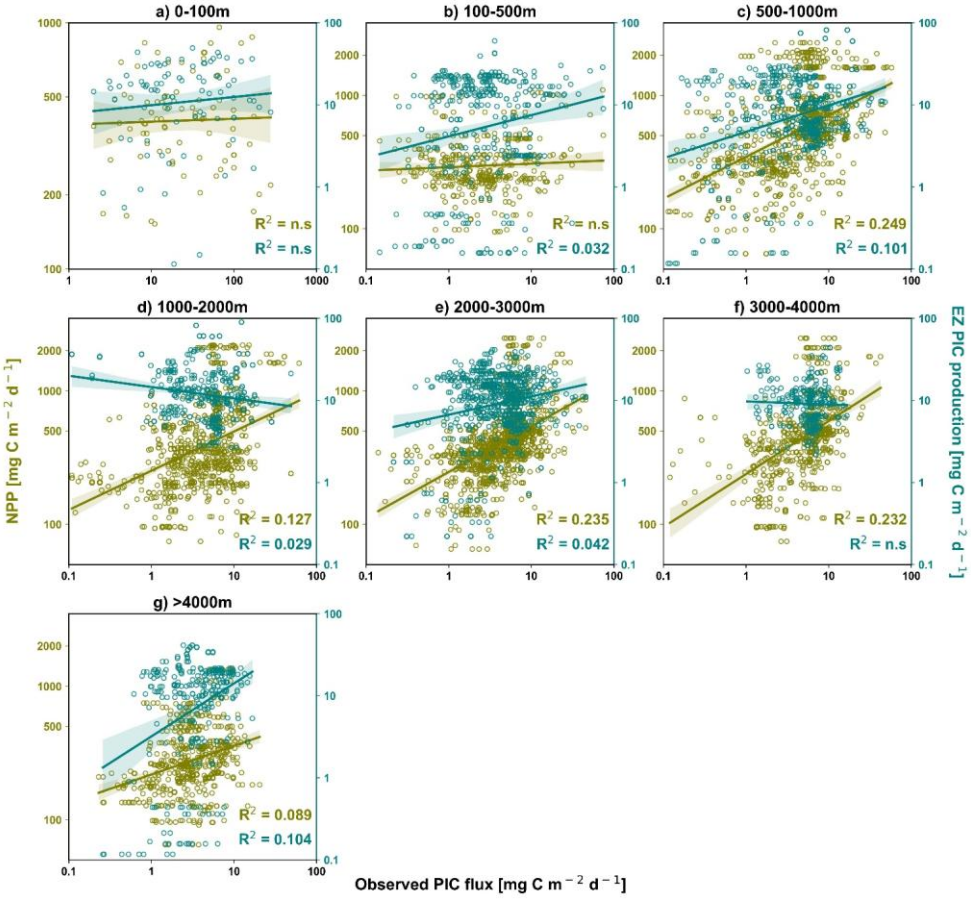

Figure 5: Matchup between observed sediment traps PIC flux (x-axis, mg PIC m^{-2} d^{-1}) and NPP (mg POC m^{-2} d^{-1}) in green, and satellite-derived PIC production (mg PIC m^{-2} d^{-1}) in blue (Hopkins et Balch, 2018 model). The different windows correspond to the different layers of depth. Non-significant correlations (p-value > 0.5, Pearson test) are indicated by "n.s.".

a mis en forme : Police :Arial

a mis en forme : Police :Arial, 9 pt

a mis en forme : Police :Arial

a mis en forme : Police :Arial

3.4. Correlation between EZ PIC production and deep PIC flux

Most of the RECCAP2 biogeochemical regions have no observations of PIC flux or are insufficient to perform correlation in shallow waters (0-100m depth). PIC flux established in shallow waters (0-100m depth) in the North Atlantic was collected during the productive period (May, June, July and August) and does not reflect the EZ PIC production seasonal variation (a non-significant correlation between EZ PIC production and PIC flux has been established, see Table S4). At the global scale, the linear regression and correlation test between EZ PIC production and PIC flux are displayed for the 6 layers of depth ~~(100-500m, 500-1000m, 1000-2000m, 2000-3000m, 3000-4000m and > 4000m)~~ and regarding the RECCAP2 biogeochemical regions in the Fig. 6 (see Table S4, for the linear regression parameters). At the global scale that the EZ PIC production is not correlated with PIC flux in the upper ocean. However, considering distinct oceanic bioregions (RECCAP2, Fig. 6), in the mesopelagic layer and deeper, significant correlations between EZ PIC production and deep PIC flux are observed in the North Atlantic (100~~-500m, 500-1000m, 1000-2000m, 2000-3000m, 3000-4000m and >~~ to 4000m) and the Southern Ocean (100-500m and 1000-2000m). North Indian Ocean regions (subtropical areas) are also characterized by PIC production positively correlated with deep PIC flux (~~500-1000m, 1000-2000m, 2000-3000m and 3000-~~500to 4000m, Fig. 6).

a mis en forme : Retrait : Gauche : 0 cm, Suspendu : 0,63 cm

a mis en forme : Police :Arial

a mis en forme : Police :Arial

a mis en forme : Police :Arial

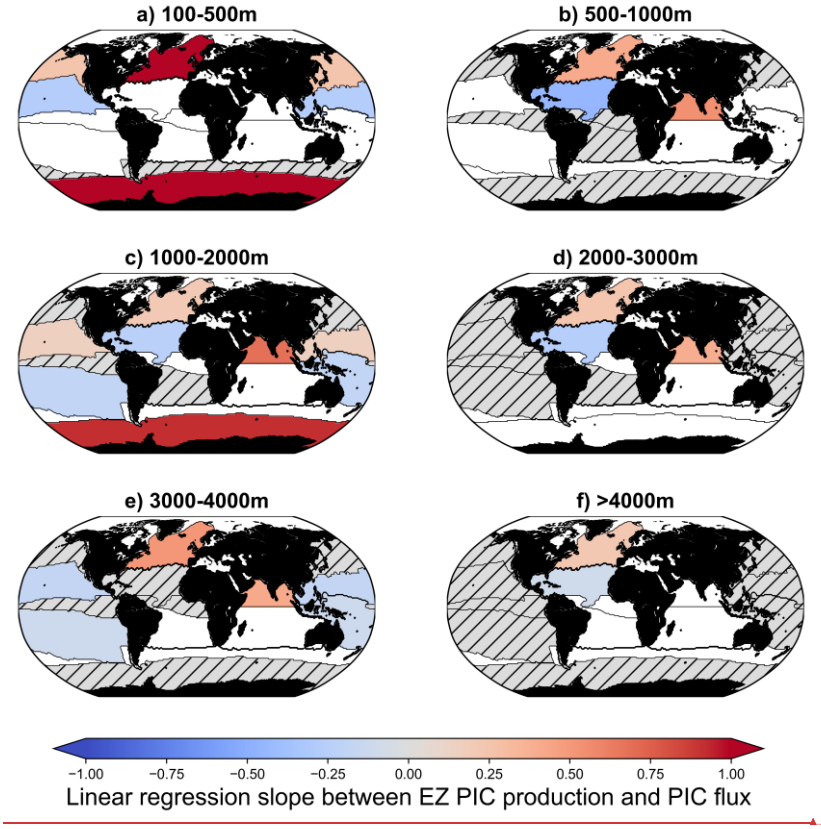

Figure 6: Map of linear regression slope between EZ PIC production and PIC flux according to the RECCAP2 regions and depth layers. Hatched grey areas correspond to regions and/or depths where the correlation coefficient is non-significant at a 95 % threshold (p-value < 0.05). White areas correspond to regions where no data are available.

The PIC export efficiency (PIC E_{eff}) corresponds to the PIC export flux divided by the EZ PIC production. A latitudinal variability trend could be overlapped to both NPP and PIC production seasonal bias (Fig. 7a). Regions above 40°, are characterized by higher PIC E_{eff} and lower PIC T_{eff} compared to subtropics and equatorial areas (Fig. 7a). The higher PIC production seasonal bias in the euphotic layer coincides with higher normalized PIC E_{eff}, but lower PIC T_{eff} (Fig. 7a). The model output of Nowicki et al. (2022), estimated that the contribution to the gravitational carbon pump of zooplankton fecal pellets and sinking phytoplankton aggregates were respectively of 85% and 15%,

a mis en forme : Police :Arial

(Nowicki et al., 2022). Once mapped of 1° by 1° grid map, zooplankton fecal pellets and sinking phytoplankton aggregates contribution are characterized by a significant latitudinal pattern (Fig. 7 in Nowicki et al., 2022). When mapped onto a 1° × 1° grid, the contributions of zooplankton fecal pellets and sinking phytoplankton aggregates exhibit a significant latitudinal pattern (Fig. 7 in Nowicki et al., 2022). The seasonality of NPP and PIC production can be overlapped with ~~aggregates's~~aggregates' contribution to the gravitational pump (estimated by Nowicki et al., 2022), as shown in Fig. 7b. The contribution of fecal pellets to the export (estimated by Nowicki et al., 2022) increases continuously from 40° to the equator, while aggregates' contribution to the export decreases. The higher contribution of fecal pellets to the export coincides with low normalized PIC E_{eff}, but high PIC T_{eff} (Fig. 7b).

a mis en forme : Police :Arial

a mis en forme : Police :Arial

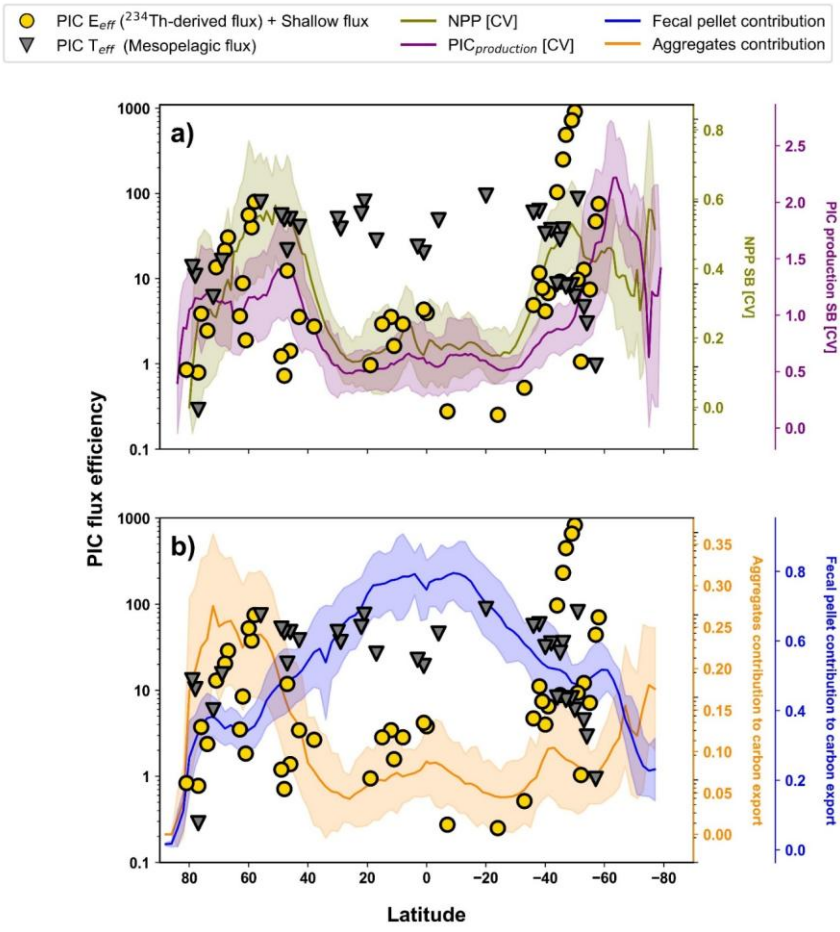

Figure 7: a) Annual PIC production seasonal bias (C.V) in purple and NPP seasonal bias (C.V) in green. Depicted in the left y-axis: The yellow circles represent the latitudinal annual mean PIC Export efficiency (PIC E_{eff}) from shallow sediment traps (0-100m) and ^{234}Th-derived flux over the latitude (x-axis). The grey triangles represent the latitudinal annual mean PIC Transfert efficiency (PIC T_{eff}) from mesopelagic sediment traps (100-1000m). b) Annual Fecal pellets contribution to the total carbon export (Nowicki et al., 2022) in blue and Annual aggregates contribution to the total carbon export (Nowicki et al., 2022) in orange. Depicted in the left y-axis: The yellow circles represent the latitudinal annual mean PIC Export efficiency (PIC E_{eff}) from shallow sediment traps (0-100m) and ^{234}Th-derived flux over the latitude (x-axis). The grey triangles represent the latitudinal annual mean PIC Transfert efficiency (PIC T_{eff}) from mesopelagic sediment traps (100-1000m).

a mis en forme : Police :Arial

a mis en forme : Police :Arial, 12 pt

4. Discussion

~~The fraction of phytoplankton exported production that is remineralized, is mainly influenced by ecosystem structure, which is related to the seasonal amplitude in NPP. Bloom of diatoms and coccolithophores (e.g. *Gephyrocapsa (Emiliania) huxleyi*), which are expected to cause intense particle sedimentation, take place mostly in in areas associated with high annual mean and amplitude of NPP, while nanoplankton/picoplankton global production are dominant in oligotrophic areas associated with low annual amplitude of NPP (Lima et al., 2014). The 'ballast effect hypothesis' induced by the inclusion of biominerals (calcite and biogenic silica) has been considered for a long time to boost the particle export efficiency (PE_{eff}), which corresponds to the proportion of primary production that is exported from the surface ocean. In the present study, the PIC E_{eff} (which corresponds to the proportion of PIC production that is exported from the surface ocean) is commonly higher above 40°N and below 40°S (temperate and subpolar oceanic regions), while the PIC T_{eff} (which corresponding to the proportion of exported PIC that reaches the deep ocean), is higher between 40°N and 40°S (subtropics), and follow the pattern than zooplankton fecal pellet contribution to the gravitational pump (Fig. 7). Considering, particles type contribution to the gravitational pump (estimated by Nowicki et al., 2022), phytoplankton aggregates could enhance the PIC E_{eff} while zooplankton fecal pellet could enhance the PIC T_{eff}. The rest of the discussion aims to identify which processes may be involved.~~

~~4.1.~~ 4.1. Mesopelagic PIC ~~flux & ballast effect hypothesis~~Flux and Ballast Effect Hypothesis

The ballast hypothesis ~~is derived~~originates from correlations between POC flux and mineral fluxes (~~opale~~opal and ~~$CaCO_3$~~$CaCO_3$) in deep sediment traps (Klaas and Archer, 2002). However, ~~it has been demonstrated that~~ ~~$CaCO_3$~~$CaCO_3$ export flux in the upper ocean ~~is~~does not ~~correlated~~correlate with ~~the~~ transfer efficiency (Henson et al., 2012~~). These points suggest~~), suggesting that ~~the association of $CaCO_3$ and POC~~ $CaCO_3$ does not ~~decrease the~~significantly protect POC from degradation ~~via a ballasting effect~~ at mesopelagic depths. ~~Indeed, Henson et al. (2012) concluded that ecosystem~~Ecosystem structure ~~is the key factor controlling the efficiency of~~, rather than mineral ballast, might be the primary control on the biological carbon pump~~, rather than the ballast effect induced by $CaCO_3$~~. François et al. (2002) ~~hypothesized~~proposed the ~~"~~"packaging ~~factor"~~factor" theory, ~~explaining~~suggesting that ~~high $CaCO_3$~~highly $CaCO_3$-productive systems ~~(relative to opal)~~ also contain organisms that produce sinking fecal pellets ~~capable of~~, which efficiently ~~delivering~~deliver organic carbon to deep waters (e.g ~~model from~~, Nowicki et al., 2022). In ~~Subtropics~~subtropical and equatorial upwelling regions, ~~the~~ export flux is not always associated with mineral ~~ballasts~~ballast (Le Moigne et al., ~~2014), while François et al.' packaging factor would suggest the opposite. These statements highlight the great~~2014), highlighting spatial variability ~~of~~in biomineral inclusion ~~into sinking particles, which argue in favour~~and supporting the role of ecosystem structure and phytoplankton phenology.

~~The results presented in this study demonstrates at the~~ On a global scale, our results demonstrate that ~~the~~ EZ PIC production is not correlated with PIC flux in the upper ocean. However, ~~considering distinct oceanic~~in specific bioregions (RECCAP2), ~~in the mesopelagic layer and deeper,~~ significant correlations exist between EZ PIC production and deep PIC flux ~~are observed in the~~ (North Atlantic ~~and the~~, Southern Ocean~~. These correlations are observed on every layer of depth and present the best R^2 coefficient (Table S4).~~, and North Indian Ocean ~~regions (subtropical areas) are also~~

a mis en forme : Police :Arial
a mis en forme : Retrait : Gauche : 0 cm, Suspendu : 0,63 cm
a mis en forme ...
a mis en forme : Sans numérotation ni puces
a mis en forme ...
a mis en forme ...
a mis en forme ...
a mis en forme : Police :Arial, Anglais (États-Unis)
a mis en forme ...

~~characterized by PIC production positively correlated with deep PIC flux (Fig. ;~~ Fig. 6~~). This evaluation demonstrates;~~ Table S4). These observations suggest that ~~at the global scale,~~ ecosystem structure and ~~phytoplankton~~ phenology ~~should be~~are more ~~of a determining factor for the PIC E_{eff} and PIC T_{eff} than the ballast effect. The hypothetic processes behind theses variability are discussed in the following part of this section, regarding the planktonic functional composition and the phenological dynamic~~important than the ballast effect in controlling PIC E_{eff} and PIC T_{eff}.

4.2. Taxa ~~contribution~~Contribution to ~~global~~Global PIC ~~stock~~Stock and ~~production~~Production

~~There is large uncertainty in total $CaCO_3$ production in the water column, with current~~ Global $CaCO_3$ production estimates remain uncertain, ranging ~~between~~from 0.7 ~~to~~ 4.7 Pg C yr^{-1} (Berelson et al., 2007; Buitenhuis et al., 2019; Lee, 2001). ~~The relative contribution of~~ Contributions from coccolithophores, foraminifers, and pteropods ~~to global production is also a big source of uncertainty. Bednaršek et al., (2012), estimated that pteropods' global annual biomass production was 5 times higher than foraminifers, but 1.5 to 3 times lower than coccolithophores (based on Balch et al., 2007, Knecht et al., 2023). According to estimates based on mechanistic modelling studies, Gangstø et al. (2008), calculated a total net pteropods $CaCO_3$ production of~~vary widely. Pteropods are estimated to contribute 0.87–4.2 Pg C yr^{-1}, representing 20–~~42~~ 89% of ~~the~~ global ~~$CaCO_3$ budget ($CaCO_3$~~ production (Gangstø et al., 2008; Lebrato et al., 2010~~). Then;~~ Buitenhuis et al., ~~(~~2019~~), still through mechanistic models, evaluated a global $CaCO_3$ production by pteropods of 4.2 Pg C yr^{-1} (89% of CaCO3 total production). Concerning the foraminifers, Schiebel (2002), estimated a variability in global foraminifers $CaCO_3$ production ranging from~~). Foraminifers contribute 0.036 ~~to~~ –0.~~065~~14 Pg C ~~y^{-1}, representing yr^{-1}~~, corresponding to 2–4% of ~~$CaCO_3$ total~~global $CaCO_3$ production (Schiebel, 2002; Lebrato et al., 2010~~). In the work of;~~ Buitenhuis et al., ~~(~~2019~~), the global foraminifers $CaCO_3$ production was estimated to be 0.14 Pg C yr^{-1} (3% of $CaCO_3$ total production). However, the relative production rate of pteropods and foraminifers compared to coccolithophore at global scale is not evaluated in this study and remain uncertain. However,~~). Coccolithophores are estimated to account for ~90% of $CaCO_3$ production (Ziveri et al~~. (2023) showed that coccolithophore represented ~ 90% of total $CaCO_3$ production in the North Pacific Ocean, while pteropods and foraminifers played a secondary role.~~

~~Significant proportion of foraminifers and pteropods are recovered inside deep~~., 2023; Kruijt et al., 2026). Deep sediment traps recover significant amounts of foraminifers and pteropods (Table 1 ~~& Fg.~~; Fig. 3 in Neukermans et al., 2023), whereas ~~coccolithophore~~coccolithophores dominate ~~the surface stranding stock and production. This observation remains unsolved and highlights a lack of understanding within the community. Potential processes are explored in the rest of this discussion.~~surface stocks and production. These observations remain poorly understood in terms of taxon-specific contributions and highlight the need for additional proof-of-concept and process-based studies to better quantify ecosystem-specific controls on PIC production and export. This study demonstrates that, at the global scale, coccolithophores dominate the PIC standing stock. Moreover, seasonal variability in coccolithophore production and biomass appears to play a central role in regulating PIC export efficiency (Fig. 7).

a mis en forme ...

4.3. ~~4.3. Mesopelagic PIC flux "biological gatekeeper"~~

Influence of Ecosystem Structure on PIC Export

The fraction of exported phytoplankton production that is remineralized is mainly influenced by ecosystem structure, which is linked to the seasonal amplitude of NPP (Fig. 7a). Blooms of diatoms and coccolithophores (e.g., *G. huxleyi*), which are expected to induce intense particle sedimentation, occur mostly in regions with high annual mean NPP and large seasonal amplitudes (Fig. 7a). In contrast, nanoplankton and picoplankton dominate global production in oligotrophic areas (low latitudes) characterized by low seasonal NPP amplitude (Lima et al., 2014). The ballast effect hypothesis, driven by biomineral inclusion (calcite and biogenic silica), has long been considered a mechanism enhancing particle export efficiency (PE_{eff}). In this study, PIC export efficiency (PIC E_{eff}; the proportion of PIC production exported from the surface) is generally higher north of 40°N and south of 40°S (temperate and subpolar regions). PIC transfer efficiency (PIC T_{eff}; the proportion of exported PIC reaching the deep ocean) is higher between 40°N and 40°S (subtropical regions) and exhibits a pattern like that of zooplankton fecal pellet contributions to the gravitational pump (Fig. 7b). Considering the main particle types involved in the gravitational pump (Nowicki et al., 2022), phytoplankton aggregates may enhance PIC E_{eff}, whereas zooplankton fecal pellets may enhance PIC T_{eff}. The following sections explore the mechanisms underlying these patterns.

4.4. ~~:~~ "Biological Gatekeeper" of the mesopelagic PIC Flux

4.4.1. Packaging Factor and Aggregate Contribution

The packaging ~~factor'~~factor theory ~~hypothesized by (~~François et al. ~~(~~., 2002~~),~~ suggests that ~~subtropics~~subtropical and equatorial ~~areas (CaCO$_3$-dominated ecosystem) are associated with~~ $CaCO_3$-rich ecosystems produce fast ~~-~~sinking fecal pellets ~~production and so high PIC export flux. Regarding the particles' dependant export output model of Nowicki et al. (2022) (Fig. 7), the relative contribution of fecal pellet to carbon~~ , thereby enhancing PIC export ~~flux is higher in subtropics~~. In this study, the particle-dependent export model (Nowicki et al., 2022; Fig. 7b) shows that fecal pellet contributions are higher in these $CaCO_3$-rich ecosystems (subtropical and equatorial ~~areas, compared to aggregates contribution.~~regions). However, observed PIC ~~export flux and deeper flux in our dataset~~fluxes are ~~globally~~ lower in ~~these~~subtropical and equatorial regions ~~(~~despite higher ~~PIC~~ production, ~~see Fig. 7), which is~~challenging the ~~opposite of the idea~~hypothesis that $CaCO_3$ packaged ~~$CaCO_3$ into the~~in fecal ~~pellet~~pellets is protected from dissolution. ~~Regarding the Aggregate's contribution to carbon export flux (Fig. 7), opal~~Opal-dominated systems (~~Temperate and sub-Polar ecosystems), are associated with~~temperate and subpolar regions) exhibit high PIC ~~flux, which is also in contradiction with the 'packaging theory'~~fluxes, suggesting ~~highly~~that labile ~~formed~~ aggregates ~~(susceptible to be easily disaggregated and remineralized). These aggregates could result in higher PIC turnover rate that~~may also enhance PIC transfer and export efficiency (PIC E_{eff}~~.~~). Overall, PIC production in the euphotic layer ~~is~~ appears to be decoupled from PIC export and transfer efficiencies (PIC E_{eff}~~. As well as~~ and PIC T_{eff} ~~through the mesopelagic layer.~~). Upper-ocean PIC loss ~~in the upper ocean is generally~~is primarily attributed to biologically mediated dissolution (Morse et al., 2006; Friis et al., 2006; Buitenhuis et al., 2019; Sulpis et al., 2021~~;~~ ; Dean et al., 2024). ~~Zooplankton~~ Although zooplankton and bacterial ~~activities~~activity decrease with depth (Hernández-León et al., 2020), ~~hence, intense zooplankton grazing and potential mediated PIC dissolution~~

a mis en forme ...

~~should occur in the~~ epipelagic and mesopelagic ~~layer. However, once the $CaCO_3$ is packaged into aggregates or fecal pellets, it should be protected from surrounding seawater and associated dissolution process, regardless of the respective depths of calcite and aragonite saturation. In that way, packaged $CaCO_3$ into aggregates of fecal pellet that settle below the saturation depth should be protected from surrounding seawater. However, zooplankton grazing could also induce aggregate fragmentation in the epipelagic and mesopelagic layers, which could be responsible for the~~grazing still appears to contribute to PIC loss ~~of PIC in shallow waters (Toullec et al., 2019 and references in there).~~

4.4.2. Hypothetical Processes of Biological-Mediated PIC Dissolution

~~**Heterotrophic4.3.1. Hypothetic processes of biological-mediated PIC dissolution**~~

~~In 2011, Bisset et al. observed that the heterotrophic~~ bacteria ~~colonising calcium carbonate~~colonizing $CaCO_3$ particles ~~(foraminifers and oyster shells) did not cause any apparent~~appear to induce minimal dissolution, suggesting a limited role in PIC loss during sinking (Bissett et al., 2011). ~~More recently, it has been shown that~~Similarly, the increase in hydrostatic pressure ~~with depth during the sedimentation of *Gephyrocapsa (Emiliania)*~~experienced by *G. huxleyi* aggregates during sedimentation does not ~~seem to modify the~~ significantly enhance calcite dissolution ~~of calcite or the remineralisation of POC~~ (Tamburini et al., 2021). ~~However, the community of bacteria colonising the aggregates, as well as the consumption of O_2, was strongly reduced with pressure, suggesting a potential preservation of PIC~~Experimental and ~~POC in the sediment thanks to the sinking of aggregates.~~

~~Several~~modeling studies ~~have even shown very slight losses of~~also show that calcite ~~after~~is largely preserved during zooplankton gut passage, ~~which contrasts with the observation of well preserved coccoliths within zooplankton fecal pellets~~with dissolution generally low or negligible across various species and conditions (Harris, 1994; Honjo, 1976; ~~Honjo and Roman, 1978;~~ Roth et al., 1975; ~~Samtleben and Bickert, 1990). Indeed, numerical models using a timeframe and pH inside copepod guts suggest a moderate calcite dissolution inside the gut (~~Langer et al., 2007; Jansen and Wolf-Gladrow, 2001~~). Langer et al. (2007) observed that calcite dissolution during copepod gut passage was below 8% of the weight of the coccoliths of *Calcidiscus leptoporus* inside fecal pellets, but these coccoliths were intact and showed no evidence of any dissolution. In addition,~~ Antia et al. (., 2008~~) successfully observed that coccolith dissolution/fragmentation occurs inside microzooplankton vacuoles (also recently observed by Dean et al., 2024), but not after copepod guts passage (also described in;~~ Toullec et al., 2022~~). However, PIC E_{eff} is higher at high latitude where fecal pellet contribution to~~; Dean et al., 2024). Despite lower contributions of fecal pellets to the gravitational pump ~~is lower (Fig.~~ at high latitudes (Fig. 7b), PIC export efficiency (PIC E_{eff}) remains elevated in these regions (temperate and subpolar areas), suggesting that additional factors, likely related to ~~7b). This result suggests more complex mechanism and implication of~~ plankton community composition and phenology ~~into the PIC E_{eff} control (see sections~~, play an important role in controlling PIC preservation and export.

4.5. Ecosystem control on PIC flux

~~4.4.3. and Fig. 7). In addition, PIC E_{eff} is higher at high latitude where phytoplankton aggregates contribution to gravitational pump is also higher (Fig. 7b and c), which suggest implication seasonal phytoplankton phenology.~~

a mis en forme : Police :Arial, Anglais (États-Unis)

4.3.2. The biogeographical pattern of zooplankton-mediated dissolution

Two experimental studies demonstrated that microzooplankton vacuole induce PIC dissolution (Antia et al., 2008; Dean et al., 2024). Microzooplankton (< 200 µm, dominated by protists) regulate) play a central role in regulating primary producer biomass and particulate organicfacilitating carbon transfer through the food web, where a fraction could then be exported asexport via fecal pelletvacuoles or aggregates (McNair et al., 2021). The contributions of microzooplankton grazing to the ocean's biological carbon remineralization are considered as the same magnitude as bacterial respiration (; Calbet and Landry, 2004). However, ecosystemic differences in microzooplankton grazing/particle export flux or trophic structure have been largely underestimated within biogeochemical models that seek to predict the microbial community's role in the oceanic carbon flux.

The percentage Their grazing intensity exhibits strong latitudinal variation, ranging from 59% of annual primary production grazed by microzooplankton increases with temperature, such as in open oceans, microzooplankton consumption varies from 59% for temperate subpolar and polar systemsregions to 75% forin tropical subtropical regions (Calbet and Landry, 2004). This latitudinal variation of microzooplankton grazing pressure could partially explain the PIC E_{eff} and PIC T_{eff} observed (Fig. 7). Annual higher grazing rates by microzooplankton are also expected in sub-tropical regions due to a low seasonal bias (Fig. 7a), leading to continuous grazing pressure from microzooplankton. This idea is also supported by the contribution of fecal pellet to the gravitational particles flux (Fig. 7b). At the end of the North Atlantic phytoplankton bloomsThese patterns align with the observed latitudinal distribution of PIC export efficiency (PIC E_{eff}) and PIC transfer efficiency (PIC T_{eff}) (Fig. 7). In the North Atlantic, microzooplankton consume the equivalent of 100–800% of their body carbon each day, which is more than an order of magnitude higher than copepods. Microzooplankton 288–589 mg C m^{-2} day^{-1} in the mixed layer grazed between 288 and 589 mg C m^{-2} day^{-1} and accounted for between 39 and 115% of the phytoplankton production In the North-Eastern Atlantic during mid-summer (, representing 39–115% of local phytoplankton production (Burkill et al., 1993).

4.3.3. PIC production timing of), highlighting their substantial contribution to particle processing and carbon flux pathway

4.3.3.1. Zooplankton impact on PIC dissolution and/or conservation

Irigoien et al. (2005) hypothesized that blooming species are capable of escaping control by. Blooming coccolithophores, such as *G. huxleyi*, can temporarily escape microzooplankton grazing during bloom onset through a combination of predation avoidance mechanisms (e.g. colonies, largertraits, including colony formation, increased cell size, spines, and toxic compounds) at the beginning of the bloom (Irigoien et al., 2005). In a temperate ecosystem, where the season variability is a determinant for PIC export flux (see Fig. 7), the coccolithophore blooms, by the large abundance of $CaCO_3$ coccoliths could be also considered as a predation avoidance mechanism (or toxin production (Irigoien et al., 2005; Monteiro et al., 2016). By this way, blooming coccolithophores such as *Gephyrocapsa (Emiliania) huxleyi* could produce too much biomass that microzooplankton grazing pressure won't be significantly sufficient to dissolve the $CaCO_3$ coccoliths in their acid vacuole. On the opposite, in subtropics and equatorial ecosystems, the annual constant coccolithophore biomass (low seasonal bias, see Fig. 7) regarding the annual consistent microzooplankton grazing pressure, coccoliths may not constitute a sufficient predation avoidance mechanism, and so could be continuously dissolved inside microzooplankton acid vacuole (Antia et al., 2008, Dean et al., 2024). Coccolithophore blooming conditions could indeed interfere with predator-prey control, permitting massive particle sinking flux thanks to aggregation formation and repackaging by mesozooplankton (e.g.:

a mis en forme : Police :Arial, Anglais (États-Unis)

copepods and larvaceans). Moreover, large zooplankton (e.g. *Calanus* spp.) graze on microzooplankton, which could significantly reduce the microzooplankton community biomass. Indeed, the mesocosm experiment demonstrated that large copepod (*Calanus finmarchicus*) ingestion rates Conversely, subtropical and equatorial regions, characterized by low seasonal variability in coccolithophore biomass and continuous grazing pressure, experience sustained PIC loss, possibly due to dissolution within microzooplankton vacuoles (Antia et al., 2008; Dean et al., 2024). Large zooplankton may indirectly enhance PIC preservation by suppressing microzooplankton biomass and repackaging coccoliths into fast-sinking fecal pellets (Nejstgaard et al., 1994). Indeed, a mesocosm study demonstrated that ingestion rates of the large copepod *Calanus finmarchicus* were similar during blooms of diatoms and E*G. huxleyi* (Nejstgaard et al., 1994). However, *C. finmarchicus* biomass increased 3 timesthreefold more in mesocosms dominated by E*G. huxleyi* compared to mesocosms with diatom bloomsthose dominated by diatoms at similar algal biomass (Nejstgaard et al., 1994). The authors suggested that during bloom conditions, copepods "preferentially" graze on the microzooplankton (Nejstgaard et al., 1994). The incorporation of coccoliths insideinto large fecal pellets (produced by mesozooplankton) is the result oflikely results from passive, non-selective feeding behaviourbehavior (e.g. current feeding, see detail below), and not necessarily), rather than from selective grazing on coccolithophores. Our dataset demonstrated that in the North Atlantic (NA), the linear regression slope between PIC production and PIC flux at different layers of depth is reveals a positive, meaning that the more PIC is produced, the more PIC flux is (Fig. 6). This positive relation is observed at every layer of depth considered in this study. During North Atlantic phytoplankton bloom phenology, grazing by microzooplankton increased when the bloom declined (typically at the end of June; Grifford et al., 1995). Microzooplankton consume up to 100% of potential daily chlorophyll *a* production at the end of the bloom (Gifford et al., 1995).

This study demonstrates a stronger correlation between NPP and PIC flux compared to PIC production and PIC flux in the North Atlantic across all depth layers (Fig. 5). At the global scale, a positive relationship between average net primary production and6), emphasizing the role of zooplankton biomass is observed in the epi-, meso-, and bathypelagic layers -mediated carbon transfer (Hernández-León et al., 2020). Moreover, the study of Hernández-León et al. (2020) suggests that this relationship could enhance the organic carbon transfer to the deep ocean (fecal pellet and excretion) and deep remineralization supported by an active carbon transport process associated with vertical zooplankton migration.

4.3.3.2. Zooplankton functional groups and dissolution pattern

A recent work based on global zooplankton data set and habitat modelling suggests that distinct copepod functional traits (e.g.: body size, feeding behaviour) are associated with differentvary among bioregions (Benedetti et al., 2023). In this study, the authors described), temperate and sub-polarsubpolar regions are dominated by large copepods, represented by detritivores/, detritivorous or omnivorous species and associated with passive feeding modescopepods that feed passively (current-feeders or cruise-feeders.; Fig. 5 in Benedetti et al., 2023). On the other hand, subtropics), whereas subtropical and equatorial upwellingregions are dominated by smaller copepods (2—2.5 mm), represented by carnivorous species and preferentially associated with active feeding modescopepods that feed actively (ambush-feeders and or current-ambush-feeders, see Fig. 5 in Benedetti et al., 2023). The concepts behind this aspect are highlighted in Fig. 8. Several studies showed grazing characteristics associated with zooplankton functional groups induce a control on the biomass and diversity of other functional groups and phytoplankton biomass as well, with consequences for global biogeochemical cycles). Grazing by these distinct functional groups shapes phytoplankton biomass and community structure, ultimately

a mis en forme ...

a mis en forme ...

a mis en forme ...

a mis en forme : Police :Arial, Couleur de police : Automatique, Anglais (États-Unis)

a mis en forme ...

influencing the efficiency and depth of PIC export (Le Quéré et al., 2016; Vallina et al., 2014~~). The present study hypothesizes that zooplankton functional groups could control the PIC export efficiency and transfer efficiency, probably mediated by guts and vacuoles dissolution of $CaCO_3$. A summary of the hypothetic mechanism is displayed in Fig. 8. In temperate areas, large copepods (e.g. *Calanus* spp.) could apply strong grazing pressure on microzooplankton (Nejstgaard et al., 1997, 1994), which could induce a trophic cascade (Wassmann, 1998), this trophic cascade is expected to be season dependent (blooming event, Fig 8). Indeed, it has been demonstrated that high trophic levels indirectly affect microbial ecosystems (Leising et al., 2005; Zöllner et al., 2009). The present study suggests that~~; Fig. 8). The present study suggests that, in temperate and subpolar ecosystems, large copepods ~~could increase the~~may enhance PIC export ~~flux~~ efficiency in ~~2 different~~two ways: (1) ~~Repackage~~by repackaging coccoliths into fecal ~~pellet (~~pellets through passive current feeding~~).~~; and (2) ~~Apply a~~by exerting strong ~~enough~~ grazing pressure on microzooplankton, ~~which could~~thereby indirectly ~~reduce $CaCO_3$~~ reducing $CaCO_3$-mediated dissolution ~~by~~within microzooplankton vacuoles (Dean et al., 2024~~;~~ Fig. 8). ~~On~~ In contrast, marine snow aggregates may create microenvironments that promote PIC dissolution in the ~~other hand, in subtropical areas, which is less seasonal, planktonic ecosystems is more complex (Chaffron~~mesopelagic layer, potentially explaining the observed decrease from PIC E_{eff} to PIC T_{eff}~~ et al., 2021). In subtropical areas, grazing rate are higher during daylight (annually) while they are diffuse~~ in temperate ~~productive areas.~~ecosystems (Fig. 8). Subtropical ~~areas were more~~regions, on the other hand, exhibit continuous grazing, efficient ~~at~~nutrient recycling, and more complex food webs. Microzooplankton strongly regulate primary producer biomass and particulate organic carbon transfer, a fraction of which may subsequently be exported as fecal pellets or aggregates (McNair et al., 2021)~~, and using nutrients through phytoplankton, while the energy transfer efficiency from nutrients to mesozooplankton appeared more efficient in temperate productive waters (Armengol et al., 2019). Shorter food web may be more efficient in energy transfer towards upper food web levels in temperate productive regions and could be the potential driver of PIC export efficiency (Fig. 8~~This ecological context may favor $CaCO_3$-mediated dissolution within microzooplankton vacuoles (Fig. 8), potentially reducing PIC export efficiency (PIC E_{eff}).

a mis en forme : Police :Arial, Couleur de police : Automatique, Anglais (États-Unis)
a mis en forme : Police :Arial, Anglais (États-Unis)
a mis en forme : Police :Arial, Couleur de police : Automatique, Anglais (États-Unis)
a mis en forme : Police :Arial, Couleur de police : Automatique, Anglais (États-Unis)
a mis en forme : Police :Arial, Couleur de police : Automatique, Anglais (États-Unis)
a mis en forme : Police :Arial, Couleur de police : Automatique, Anglais (États-Unis)
a mis en forme : Police :Arial, Couleur de police : Automatique, Anglais (États-Unis)
a mis en forme : Police :Arial, Couleur de police : Automatique, Anglais (États-Unis)
a mis en forme : Police :Arial, Couleur de police : Automatique, Anglais (États-Unis)
a mis en forme : Police :Arial, Couleur de police : Automatique, Anglais (États-Unis)
a mis en forme : Police :Arial, Couleur de police : Automatique, Anglais (États-Unis)
a mis en forme : Police :Arial, Couleur de police : Automatique, Anglais (États-Unis)
a mis en forme : Police :Arial, Couleur de police : Automatique, Anglais (États-Unis)
a mis en forme : Police :Arial, Couleur de police : Automatique, Anglais (États-Unis)
a mis en forme : Police :Arial, Couleur de police : Automatique, Anglais (États-Unis)
a mis en forme : Police :Arial, Couleur de police : Automatique, Anglais (États-Unis)
a mis en forme : Police :Arial, Anglais (États-Unis)
a mis en forme : Police :Arial, Couleur de police : Automatique, Anglais (États-Unis)
a mis en forme ...
a mis en forme ...
a mis en forme ...
a mis en forme ...
a mis en forme : Police :Arial, Anglais (États-Unis)
a mis en forme ...

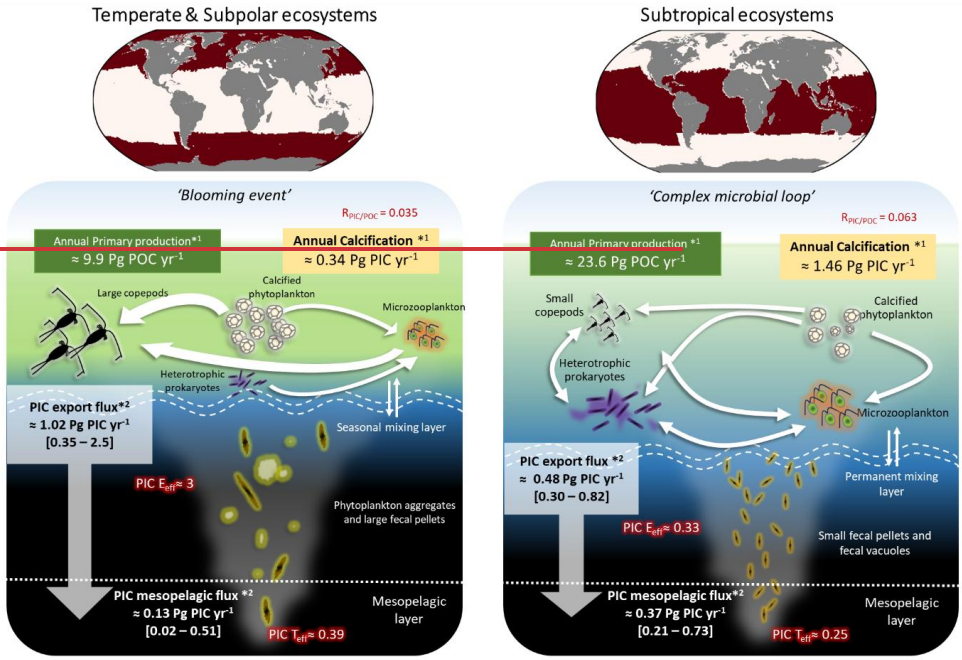

*1 Satellite based NPP, excluding continental margin (200m depth) and interior sea
*2 Estimates based on the sediment trap annual PIC flux (g C m^{-2} yr^{-1}) extended to the total surface area. Results are expressed by the median and interquartile [q25 – q75]

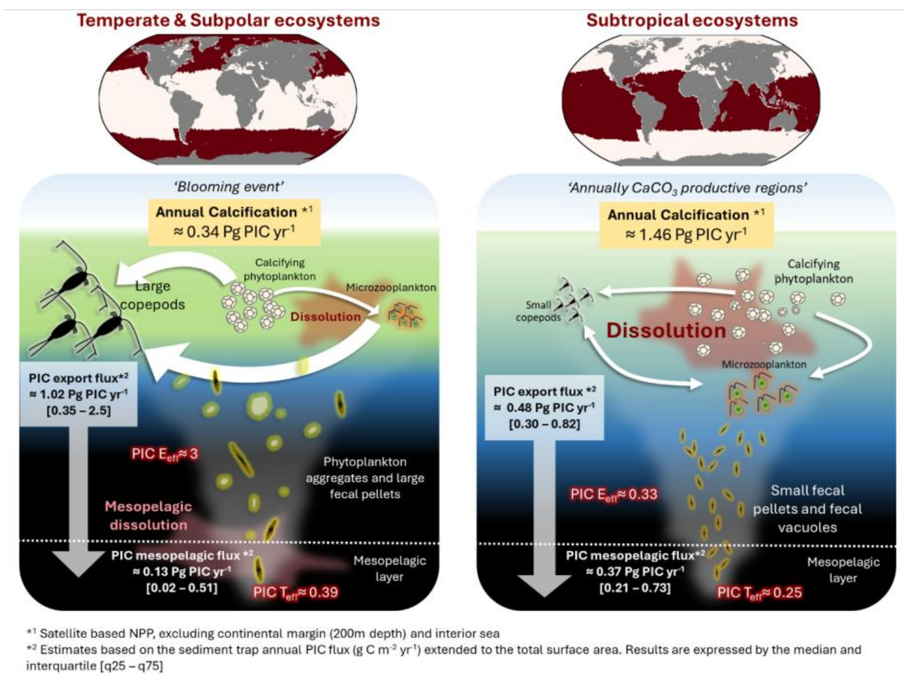

Figure 8: Synthesis of the potential PIC pathway through the water column, in two distinct ecosystems; a) Subtropical ecosystems (subtropical gyres and equatorial upwellings). b) Temperate zone (North Atlantic, North Pacific and subpolar regions). The white arrows represent the trophic transfer between the different planktonic compartments (Predator prey), and double arrow means that both compartments could be both prey and predator each other. Small copepods correspond to individual body sizes ranging from 200 µm to 2 mm; Microzooplankton (mostly protists, < 200 µm) represent the flagellates and ciliates community; Large copepods correspond to individual body sizes larger than 2 mm (mostly large calanoid). Note that microzooplankton could be heterotrophic, autotrophic or mixotrophic.

This study integrates the main conceptual frameworks currently proposed in the field to interpret the observed patterns in PIC export efficiency (PIC E_{eff}) and biologically mediated $CaCO_3$ dissolution. Our results highlight that variability in PIC E_{eff} and the mechanisms regulating $CaCO_3$ dissolution remain insufficiently constrained, particularly across contrasting biogeographical regimes. These findings underscore the need for targeted proof-of-concept and process-based studies to better quantify ecosystem-specific controls on PIC export. Improving this mechanistic understanding is essential for refining predictions of the oceanic carbon cycle under ongoing environmental changes.

a mis en forme : Police :Arial, Couleur de police : Automatique, Anglais (États-Unis)
a mis en forme : Police :Arial, Anglais (États-Unis)
a mis en forme : Police :Arial, Couleur de police : Automatique, Anglais (États-Unis)
a mis en forme : Police :Arial, Anglais (États-Unis)
a mis en forme : Police :Arial, Couleur de police : Automatique, Anglais (États-Unis)
a mis en forme : Police :Arial, Anglais (États-Unis)
a mis en forme : Police :Arial, Couleur de police : Automatique, Anglais (États-Unis)
a mis en forme : Police :Arial, Couleur de police : Automatique, Anglais (États-Unis)
a mis en forme : Police :Arial, Anglais (États-Unis)
a mis en forme : Police :Arial, Couleur de police : Automatique, Anglais (États-Unis)
a mis en forme : Police :Arial, Anglais (États-Unis)
a mis en forme : Police :Arial, Couleur de police : Automatique, Anglais (États-Unis)
a mis en forme : Police :Arial, Anglais (États-Unis)
a mis en forme : Police :Arial, Couleur de police : Automatique, Anglais (États-Unis)
a mis en forme : Police :Arial, Anglais (États-Unis)
a mis en forme : Police :Arial, Couleur de police : Automatique, Anglais (États-Unis)
a mis en forme : Police :Arial, Anglais (États-Unis)
a mis en forme : Police :Arial, Couleur de police : Automatique, Anglais (États-Unis)

5. Conclusion and perspectives

In this study, the ~~'~~"packaging ~~factor'~~factor" theory is ~~suggested to be~~ proposed as an important driver of the discrepancy between ~~the~~ estimated PIC production and ~~the~~ export flux ~~in~~across distinct oceanic regions. Despite the PIC/POC production ratio being twice as high in subtropical ~~areas~~regions compared to temperate and subpolar ~~areas, the~~regions, PIC ~~Export $_{eff}$~~export efficiency (PIC E_{eff}) is estimated ~~10 times~~to be tenfold lower and ~~the PIC Transfer $_{eff}$~~PIC transfer efficiency (PIC T_{eff}) 1.5 ~~times~~-fold lower.

~~This study suggests~~ Our results suggest that ~~the~~ zooplankton functional diversity and biogeography ~~could~~may explain the ~~different~~contrasting patterns of ~~$CaCO_3$~~$CaCO_3$ export efficiency, ~~considering different patterns of~~through differences in dissolution and ~~conservation into~~ preservation within particles. Such ~~a process~~processes could ~~significantly~~substantially contribute to ~~the~~ total downward ~~export of~~ carbon export and associated ~~nutrients.~~nutrient fluxes. However, only ~~few~~ a limited number of experimental studies have directly demonstrated the ~~actual~~ effect of zooplankton functional diversity ~~effect~~ on ~~$CaCO_3$~~$CaCO_3$ dissolution. To ~~confirm~~test and ~~complete this present study~~ refine the hypothesis proposed here, there is a strong need for experimental data and in situ observations ~~regarding~~addressing both mesozooplankton and microzooplankton grazing ~~dynamic~~dynamics and ~~$CaCO_3$ flux.~~ $CaCO_3$ fluxes.

In ~~a~~the context of surface ocean warming and acidification, phytoplankton losses due to microzooplankton grazing in eutrophic waters are expected to increase (Chen et al., 2012), ~~which could have an attenuation effect on~~ potentially attenuating the carbonate ~~pumps within~~pump in temperate regions. In addition, POC export ~~will not~~ is unlikely to respond ~~equally~~uniformly across ~~all~~ high-latitude regions to ~~possible~~ future changes in ballast availability, which ~~could~~may also ~~have consequences in~~affect the biological carbon pump (BCP-), Data ~~compilation~~compilations and model ~~output demonstrated~~outputs indicate that coccolithophores ~~generally~~ tend to ~~be~~become less calcified ~~relatively~~relative to growth ~~when the CO_2 increases~~ under increasing CO_2 concentrations (Krumhardt et al., 2017, 2019). ~~The end~~End-of-century ~~CO_2 concentrations projection result~~CO_2 projections suggest an approximately 11% ~~less~~ decline in global oceanic calcification ~~on a global scale~~ relative to preindustrial ~~CO_2~~ levels (Krumhardt et al., 2019). ~~All this implication~~Such changes in surface ocean dynamics ~~would have consequences on~~ are expected to alter the future balance of surface alkalinity ~~balance~~ and ~~CO_2~~CO_2 exchange between the ocean and atmosphere (Planchat et al., 2024; Tyrrell, 2008; Volk ~~&~~and Hoffert, 1985).

Code and Data availability. The author confirms that the data supporting the findings of this study are available within the article and its Supplement.

Author's contribution. Jordan Toullec: Conceptualization, Data curation, Formal analysis, Investigation, Methodology, Validation, Visualization, Writing original draft, study and editing.

Competing interest. The author ~~declare that they have~~declares no known competing financial interests or personal relationships that could have appeared to influence the work reported in this paper.

Financial support. Jordan Toullec worked on this study while he was a post-doctorate fellow funded by CARBOCEAN ERC project: ERC-StG2019-853516. Jordan Toullec is now a post-doctorate fellow funded by

a mis en forme : Police :Arial
a mis en forme : Retrait : Gauche : 0 cm, Suspendu : 0,63 cm
a mis en forme ...
a mis en forme ...
a mis en forme ...
a mis en forme : Espace Avant : 18 pt
a mis en forme : Police :Arial

CLIMArcTIC PPR project : *'Océan et Climat' Défi 2: Intensifier les recherches dans des océans polaires en pleine mutation et aux enjeux géostratégiques majeurs.*

6. References

Armengol, L., Calbet, A., Franchy, G., Rodríguez-Santos, A., & Hernández-León, S. Planktonic food web structure and trophic transfer efficiency along a productivity gradient in the tropical and subtropical Atlantic Ocean. Scientific reports, 9(1), 2044. 2019.

Armstrong, R. A., Lee, C., Hedges, J. I., Honjo, S., & Wakeham, S. G. A new, mechanistic model for organic carbon fluxes in the ocean based on the quantitative association of POC with ballast minerals. Deep Sea Research Part II: Topical Studies in Oceanography, 49(1-3), 219-236. 2001

Antia, A. N., Suffrian, K., Holste, L., Müller, M. N., Nejstgaard, J. C., Simonelli, P., Carotenuto, Y., and Putzeys, S.: Dissolution of coccolithophorid calcite by microzooplankton and copepod grazing, Biogeosciences discussion, https://doi.org/10.5194/bgd-5-1-2008, 2008.

Antoine, D. and Morel, A.: Oceanic primary production: 1. Adaptation of a spectral light-photosynthesis model in view of application to satellite chlorophyll observations, Global Biogeochemical Cycles, 10, 43–55, https://doi.org/10.1029/95GB02831, 1996.

Balch, W. M. and Mitchell, C.: Remote sensing algorithms for particulate inorganic carbon (PIC) and the global cycle of PIC, Earth-Science Reviews, 239, 104363, https://doi.org/10.1016/j.earscirev.2023.104363, 2023.

Balch, W. M., Kilpatrick, K. A., Holligan, P., Harbour, D., and Fernandez, E.: The 1991 coccolithophore bloom in the central North Atlantic. 2. Relating optics to coccolith concentration, Limnology and Oceanography, 41, 1684–1696, https://doi.org/10.4319/lo.1996.41.8.1684, 1996.

Balch, W. M., Gordon, H. R., Bowler, B. C., Drapeau, D. T., and Booth, E. S.: Calcium carbonate measurements in the surface global ocean based on Moderate-Resolution Imaging Spectroradiometer data, Journal of Geophysical Research: Oceans, 110, https://doi.org/10.1029/2004JC002560, 2005.

Balch, W. M., Drapeau, D. T., Bowler, B. C., Lyczskowski, E., Booth, E. S., and Alley, D.: The contribution of coccolithophores to the optical and inorganic carbon budgets during the Southern Ocean Gas Exchange Experiment: New evidence in support of the "Great Calcite Belt" hypothesis, Journal of Geophysical Research: Oceans, 116, https://doi.org/10.1029/2011JC006941, 2011.

Balch, W. M., Bowler, B. C., Drapeau, D. T., Lubelczyk, L. C., and Lyczkowski, E.: Vertical Distributions of Coccolithophores, PIC, POC, Biogenic Silica, and Chlorophyll a Throughout the Global Ocean, Global Biogeochemical Cycles, 32, 2–17, https://doi.org/10.1002/2016GB005614, 2018.

Barton, A. D., Pershing, A. J., Litchman, E., Record, N. R., Edwards, K. F., Finkel, Z. V., Kiørboe, T., and Ward, B. A.: The biogeography of marine plankton traits, Ecology Letters, 16, 522–534, https://doi.org/10.1111/ele.12063, 2013.

Bednaršek, N., Možina, J., Vogt, M., O'Brien, C., and Tarling, G. A.: The global distribution of pteropods and their contribution to carbonate and carbon biomass in the modern ocean, Earth System Science Data, 4, 167–186, https://doi.org/10.5194/essd-4-167-2012, 2012.

a mis en forme : Retrait : Gauche : 0 cm, Suspendu : 0,63 cm

Bendif, E. M., Probert, I., Archontikis, O. A., Young, J. R., Beaufort, L., Rickaby, R. E., & Filatov, D. Rapid diversification underlying the global dominance of a cosmopolitan phytoplankton. The ISME Journal, 17(4), 630-640. 2023

Benedetti, F., Wydler, J., and Vogt, M.: Copepod functional traits and groups show divergent biogeographies in the global ocean, Journal of Biogeography, 50, 8–22, https://doi.org/10.1111/jbi.14512, 2023.

Berelson, W. M., Balch, W. M., Najjar, R., Feely, R. A., Sabine, C., and Lee, K.: Relating estimates of CaCO3 production, export, and dissolution in the water column to measurements of CaCO3 rain into sediment traps and dissolution on the sea floor: A revised global carbonate budget, Global Biogeochemical Cycles, 21, https://doi.org/10.1029/2006GB002803, 2007.

Berner, R. A. and Morse, J. W.: Dissolution kinetics of calcium carbonate in sea water; IV, Theory of calcite dissolution, American Journal of Science, 274, 108–134, https://doi.org/10.2475/ajs.274.2.108, 1974.

Bissett, A., Neu, T. R., and Beer, D. de: Dissolution of Calcite in the Twilight Zone: Bacterial Control of Dissolution of Sinking Planktonic Carbonates Is Unlikely, PLOS ONE, 6, e26404, https://doi.org/10.1371/journal.pone.0026404, 2011.

Brandão, S. N., Hoppema, M., Kamenev, G. M., Karanovic, I., Riehl, T., Tanaka, H., Vital, H., Yoo, H., and Brandt, A.: Review of Ostracoda (Crustacea) living below the Carbonate Compensation Depth and the deepest record of a calcified ostracod, Progress in Oceanography, 178, 102144, https://doi.org/10.1016/j.pocean.2019.102144, 2019.

Brown, C. W., & Yoder, J. A. Coccolithophorid blooms in the global ocean. Journal of Geophysical Research: Oceans, 99(C4), 7467-7482. 1994.

Buitenhuis, E. T., Le Quéré, C., Bednaršek, N., and Schiebel, R.: Large Contribution of Pteropods to Shallow CaCO3 Export, Global Biogeochemical Cycles, 33, 458–468, https://doi.org/10.1029/2018GB006110, 2019.

Burkill, P. H., Edwards, E. S., John, A. W. G., and Sleigh, M. A.: Microzooplankton and their herbivorous activity in the northeastern Atlantic Ocean, Deep Sea Research Part II: Topical Studies in Oceanography, 40, 479–493, https://doi.org/10.1016/0967-0645(93)90028-L, 1993.

Burridge, A. K., Goetze, E., Wall-Palmer, D., Le Double, S. L., Huisman, J., and Peijnenburg, K. T. C. A.: Diversity and abundance of pteropods and heteropods along a latitudinal gradient across the Atlantic Ocean, Progress in Oceanography, 158, 213–223, https://doi.org/10.1016/j.pocean.2016.10.001, 2017.

Buesseler, K. O., Lamborg, C. H., Boyd, P. W., Lam, P. J., Trull, T. W., Bidigare, R. R., Bishop, J. K. B., Casciotti, K. L., Dehairs, Elskens, M., Honda, M., Karl, D. M., Siegel, D. A., Silver, M. W., Steinberg, D. K. Valdes, J., Van Mooy, B. & Wilson, S. Revisiting carbon flux through the ocean's twilight zone. science, 316(5824), 567-570. 2007

Calbet, A. and Landry, M. R.: Phytoplankton growth, microzooplankton grazing, and carbon cycling in marine systems, Limnology and Oceanography, 49, 51–57, https://doi.org/10.4319/lo.2004.49.1.0051, 2004.

Chaabane, S., de Garidel-Thoron, T., Meilland, J., Sulpis, O., Chalk, T. B., Brummer, G. J. A., ... & Schiebel, R.: Migrating is not enough for modern planktonic foraminifera in a changing ocean. Nature, 1-7. https://doi.org/s41586-024-08191-5, 2024.

Chaffron, S., Delage, E., Budinich, M., Vintache, D., Henry, N., Nef, C., Ardyna, M., Zayed, A. A., Junger, P. C., Galand, P. E., Lovejoy, C., Murray, A. E., Sarmento, H., Tara Oceans coordinators, Acinas, S. G., Babin, M., Iudicone, D., Jaillon, O., Karsenti, E., Wincker, P., Karp-Boss, L., Sullivan, M. B., Bowler, C., de Vargas, C. & Eveillard, D. Environmental vulnerability of the global ocean epipelagic plankton community interactome. Science Advances, 7(35), eabg1921. 2021.

Chen, B., Landry, M. R., Huang, B., and Liu, H.: Does warming enhance the effect of microzooplankton grazing on marine phytoplankton in the ocean?, Limnology and Oceanography, 57, 519–526, https://doi.org/10.4319/lo.2012.57.2.0519, 2012.

Clements, D. J., Yang, S., Weber, T., McDonnell, A. M. P., Kiko, R., Stemmann, L., and Bianchi, D.: New Estimate of Organic Carbon Export From Optical Measurements Reveals the Role of Particle Size Distribution and Export Horizon, Global Biogeochemical Cycles, 37, e2022GB007633, https://doi.org/10.1029/2022GB007633, 2023.

Dean, C. L., Harvey, E. L., Johnson, M. D., & Subhas, A. V. Microzooplankton grazing on the coccolithophore Emiliania huxleyi and its role in the global calcium carbonate cycle. Science Advances, 10(45), eadr5453. 2024

Feely, R. A., Sabine, C. L., Lee, K., Millero, F. J., Lamb, M. F., Greeley, D., ... & Wong, C. S. In situ calcium carbonate dissolution in the Pacific Ocean. Global Biogeochemical Cycles, 16(4), 91-1. 2002.

Fischer, G., Karstensen, J., Romero, O., Baumann, K.-H., Donner, B., Hefter, J., Mollenhauer, G., Iversen, M., Fiedler, B., Monteiro, I., and Körtzinger, A.: Bathypelagic particle flux signatures from a suboxic eddy in the oligotrophic tropical North Atlantic: production, sedimentation and preservation, Biogeosciences, 13, 3203–3223, https://doi.org/10.5194/bg-13-3203-2016, 2016.

Francois, R., Honjo, S., Krishfield, R., and Manganini, S.: Factors controlling the flux of organic carbon to the bathypelagic zone of the ocean, Global Biogeochemical Cycles, 16, 34-1-34–20, https://doi.org/10.1029/2001GB001722, 2002.

Friis, K., Najjar, R. G., Follows, M. J. & Dutkiewicz, S. Possible overestimation of shallow-depth calcium carbonate dissolution in the ocean. Glob. Biogeochem. Cycles https://doi.org/10.1029/2006gb002727. 2006.

Gangstø, R., Gehlen, M., Schneider, B., Bopp, L., Aumont, O., and Joos, F.: Modeling the marine aragonite cycle: changes under rising carbon dioxide and its role in shallow water $CaCO_3$ dissolution, Biogeosciences, 5, 1057–1072, https://doi.org/10.5194/bg-5-1057-2008, 2008.

Gifford, D. J., Fessenden, L. M., Garrahan, P. R., and Martin, E.: Grazing by microzooplankton and mesozooplankton in the high-latitude North Atlantic Ocean: Spring versus summer dynamics, Journal of Geophysical Research: Oceans, 100, 6665–6675, https://doi.org/10.1029/94JC00983, 1995.

Guerreiro, C. V., Baumann, K. H., Brummer, G. J. A., Valente, A., Fischer, G., Ziveri, P., Vanda, B. & Stuut, J. B. W. Carbonate fluxes by coccolithophore species between NW Africa and the Caribbean: Implications for the biological carbon pump. Limnology and Oceanography, 66(8), 3190-3208. 2021.

Harris, R. P.: Zooplankton grazing on the coccolithophore Emiliania huxleyi and its role in inorganic carbon flux, Marine Bioliogy, 119, 431–439, https://doi.org/10.1007/BF00347540, 1994.

Hauck, J., Gruber, N., Ishii, M., and Müller, J. D.: Constraining regional and global ocean carbon fluxes in RECCAP2, Copernicus Meetings, https://doi.org/10.5194/egusphere-egu23-12786, 2023.

Henson, S. A., Sanders, R., and Madsen, E.: Global patterns in efficiency of particulate organic carbon export and transfer to the deep ocean: ~~EXPORT AND TRANSFER EFFICIENCY~~Export and transfer efficiency, Global Biogeochem. Cycles, 26, n/a-n/a, https://doi.org/10.1029/2011GB004099, 2012.

Henson, S., Le Moigne, F., & Giering, S. Drivers of carbon export efficiency in the global ocean. Global biogeochemical cycles, 33(7), 891-903. 2019.

Hernández-León, S., Koppelmann, R., Fraile-Nuez, E., Bode, A., Mompeán, C., Irigoien, X., Olivar, M. P., Echevarría, F., Fernández de Puelles, M. L., González-Gordillo, J. I., Cózar, A., Acuña, J. L., Agustí, S., and Duarte, C. M.: Large deep-sea zooplankton biomass mirrors primary production in the global ocean, Nat Commun, 11, 6048, https://doi.org/10.1038/s41467-020-19875-7, 2020.

Holligan, P. M., Fernández, E., Aiken, J., Balch, W. M., Boyd, P., Burkill, P. H., Finch, M., Groom, S. B., Malin, G., Muller, K., Purdie, D. A., Robinson, C., Trees, C. C., Turner, S. M., and van der Wal, P.: A biogeochemical study of the coccolithophore, Emiliania huxleyi, in the North Atlantic, Global Biogeochemical Cycles, 7, 879–900, https://doi.org/10.1029/93GB01731, 1993.

Honjo, S.: Coccoliths: Production, transportation and sedimentation, Marine Micropaleontology, 1, 65–79, https://doi.org/10.1016/0377-8398(76)90005-0, 1976.

Honjo, S. and Roman, M.: Marine copepod fecal pellets: Production, preservation and sedimentation, Journal of Marine Research, 36, 1978.

Hopkins, J., Henson, S. A., Painter, S. C., Tyrrell, T., & Poulton, A. J. Phenological characteristics of global coccolithophore blooms. Global Biogeochemical Cycles, 29(2), 239-253. 2015.

Hopkins, J. and Balch, W. M.: A New Approach to Estimating Coccolithophore Calcification Rates From Space, Journal of Geophysical Research: Biogeosciences, 123, 1447–1459, https://doi.org/10.1002/2017JG004235, 2018.

Irigoien, X., Flynn, K. J., and Harris, R. P.: Phytoplankton blooms: a 'loophole' in microzooplankton grazing impact?, Journal of Plankton Research, 27, 313–321, https://doi.org/10.1093/plankt/fbi011, 2005.

Iversen, M. H. and Ploug, H.: Ballast minerals and the sinking carbon flux in the ocean: carbon-specific respiration rates and sinking velocity of marine snow aggregates, Biogeosciences, 7, 2613–2624, https://doi.org/10.5194/bg-7-2613-2010, 2010.

Jansen, H. and Wolf-Gladrow, D.: Carbonate dissolution in copepod guts: a numerical model, Mar. Ecol. Prog. Ser., 221, 199–207, https://doi.org/10.3354/meps221199, 2001.

Kaneko, H., Endo, H., Henry, N., Berney, C., Mahé, F., Poulain, J., Labadie, K., Beluche, O., El Hourany, R., Chaffron, S., Wincker, P., Nakamura, R., Karp-Boss, L., Boss, E., Chris Bowler, de Vargas, C., Tomii, K., and Ogata, H.: Predicting global distributions of eukaryotic plankton communities from satellite data, ISME COMMUN., 3, 1–9, https://doi.org/10.1038/s43705-023-00308-7, 2023.

Klaas, C. and Archer, D. E.: Association of sinking organic matter with various types of mineral ballast in the deep sea: Implications for the rain ratio, Global Biogeochemical Cycles, 16, 63-1-63–14, https://doi.org/10.1029/2001GB001765, 2002.

a mis en forme : Police :Arial

Knecht, N. S., Benedetti, F., Elizondo, U. H., Bednaršek, N., Chaabane, S., de Weerd, C., Peijnenburg, K. T. C. A., Schiebel, R., and Vogt, M.: The impact of zooplankton calcifiers on the marine carbon cycle, Global Biogeochemical Cycles, n/a, e2022GB007685, https://doi.org/10.1029/2022GB007685, 2023.

Kruijt, A. L., van Dijk, R., Sulpis, O., Beaufort, L., Lassus, G., Brummer, G.-J., van der Burg, A. D., Cala, B. A., Ourradi, Y., Peijnenburg, K. T. C. A., Humphreys, M. P., Chaabane, S., Sluijs, A., and Middelburg, J. J.: The contributions of various calcifying plankton to the South Atlantic calcium carbonate stock, Biogeosciences, 23, 531–563, https://doi.org/10.5194/bg-23-531-2026, 2026.

Krumhardt, K. M., Lovenduski, N. S., Iglesias-Rodriguez, M. D., and Kleypas, J. A.: Coccolithophore growth and calcification in a changing ocean, Progress in Oceanography, 159, 276–295, https://doi.org/10.1016/j.pocean.2017.10.007, 2017.

Krumhardt, K. M., Lovenduski, N. S., Long, M. C., Lévy, M., Lindsay, K., Moore, J. K., & Nissen, C. Coccolithophore growth and calcification in an acidified ocean: Insights from community Earth system model simulations. Journal of Advances in Modeling Earth Systems, 11(5), 1418-1437. 2019

Kwon, E. Y., Dunne, J. P., & Lee, K. Biological export production controls upper ocean calcium carbonate dissolution and CO2 buffer capacity. Science Advances, 10(13), eadl0779. 2024

Lacour, L., Llort, J., Briggs, N., Strutton, P. G., & Boyd, P. W. Seasonality of downward carbon export in the Pacific Southern Ocean revealed by multi-year robotic observations. Nature Communications, 14(1), 1278. 2023.

Langer, G., Nehrke, G., and Jansen, S.: Dissolution of Calcidiscus leptoporus coccoliths in copepod guts? A morphological study, Mar. Ecol. Prog. Ser., 331, 139–146, https://doi.org/10.3354/meps331139, 2007.

Lalli, C. M., & Gilmer, R. W. Pelagic snails: the biology of holoplanktonic gastropod mollusks. Stanford University Press. 1989.

Laurenceau-Cornec, E. C., Le Moigne, F. A. C., Gallinari, M., Moriceau, B., Toullec, J., Iversen, M. H., Engel, A., and De La Rocha, C. L.: New guidelines for the application of Stokes' models to the sinking velocity of marine aggregates, Limnology and Oceanography, 65, 1264–1285, https://doi.org/10.1002/lno.11388, 2020.

Le Moigne, F. A. C., Pabortsava, K., Marcinko, C. L. J., Martin, P., and Sanders, R. J.: Where is mineral ballast important for surface export of particulate organic carbon in the ocean?, Geophysical Research Letters, 41, 8460–8468, https://doi.org/10.1002/2014GL061678, 2014.

Le Quéré, C., Buitenhuis, E. T., Moriarty, R., Alvain, S., Aumont, O., Bopp, L., Chollet, S., Enright, C., Franklin, D. J., Geider, R. J., Harrison, S. P., Hirst, A. G., Larsen, S., Legendre, L., Platt, T., Prentice, I. C., Rivkin, R. B., Sailley, S., Sathyendranath, S., Stephens, N., Vogt, M., and Vallina, S. M.: Role of zooplankton dynamics for Southern Ocean phytoplankton biomass and global biogeochemical cycles, Biogeosciences, 13, 4111–4133, https://doi.org/10.5194/bg-13-4111-2016, 2016.

Lebrato, M., Iglesias-Rodríguez, D., Feely, R. A., Greeley, D., Jones, D. O. B., Suarez-Bosche, N., Lampitt, R. S., Cartes, J. E., Green, D. R. H., and Alker, B.: Global contribution of echinoderms to the marine carbon cycle: CaCO3 budget and benthic compartments, Ecological Monographs, 80, 441–467, https://doi.org/10.1890/09-0553.1, 2010.

Lee, K.: Global net community production estimated from the annual cycle of surface water total dissolved inorganic carbon, Limnology and Oceanography, 46, 1287–1297, https://doi.org/10.4319/lo.2001.46.6.1287, 2001.

a mis en forme : Police :Arial

Leising, A. W., Pierson, J. J., Halsband-Lenk, C., Horner, R., and Postel, J.: Copepod grazing during spring blooms: Can Pseudocalanus newmani induce trophic cascades?, Progress in Oceanography, 67, 406–421, https://doi.org/10.1016/j.pocean.2005.09.009, 2005.

Lima, I. D., Lam, P. J., and Doney, S. C.: Dynamics of particulate organic carbon flux in a global ocean model, Biogeosciences, 11, 1177–1198, https://doi.org/10.5194/bg-11-1177-2014, 2014.

Li, J., Liu, Z., Lin, B., Zhao, Y., Cao, J., Zhang, X., Ling. C., Ma. P. & Wu, J. Zooplankton fecal pellet characteristics and contribution to the deep-sea carbon export in the southern South China Sea. Journal of Geophysical Research: Oceans, 127(12), e2022JC019412. 2022

Millero, F. J., Lee, K., & Roche, M. Distribution of alkalinity in the surface waters of the major oceans. Marine Chemistry, 60(1-2), 111-130. 1998.

Milliman, J. D., Troy, P. J., Balch, W. M., Adams, A. K., Li, Y.-H., and Mackenzie, F. T.: Biologically mediated dissolution of calcium carbonate above the chemical lysocline?, Deep Sea Research Part I: Oceanographic Research Papers, 46, 1653–1669, https://doi.org/10.1016/S0967-0637(99)00034-5, 1999.

Monteiro, F. M., Bach, L. T., Brownlee, C., Bown, P., Rickaby, R. E. M., Poulton, A. J., Tyrrell, T., Beaufort, L., Dutkiewicz, S., Gibbs, S., Gutowska, M. A., Lee, R., Riebesell, U., Young, J., and Ridgwell, A.: Why marine phytoplankton calcify, Sci. Adv., 2, e1501822, https://doi.org/10.1126/sciadv.1501822, 2016.

Morse, J. W., Andersson, A. J. & Mackenzie, F. T. Initial responses of carbonate-rich shelf sediments to rising atmospheric pCO2 and “ocean acidification”: role of high Mg-calcites. Geochim. Cosmochim. Acta 70, 5814–5830. 2006.

Mouw, C. B., Barnett, A., McKinley, G. A., Gloege, L., and Pilcher, D.: Global ocean particulate organic carbon flux merged with satellite parameters, Earth System Science Data, 8, 531–541, https://doi.org/10.5194/essd-8-531-2016, 2016.

Nejstgaard, J., Gismervik, I., and Solberg, P.: Feeding and reproduction by Calanus finmarchicus, and microzooplankton grazing during mesocosm blooms of diatoms and the coccolithophore Emiliania huxleyi, Mar. Ecol. Prog. Ser., 147, 197–217, https://doi.org/10.3354/meps147197, 1997.

Nejstgaard, J. C., Witte, H. J., van der Wal, P., and Jacobsen, A.: Copepod grazing during a mesocosm study of an Emiliania huxleyi (Prymnesiophyceae) bloom, Sarsia, 79, 369–377, https://doi.org/10.1080/00364827.1994.10413568, 1994.

Neukermans, G., Bach, L. T., Butterley, A., Sun, Q., Claustre, H., and Fournier, G. R.: Quantitative and mechanistic understanding of the open ocean carbonate pump - perspectives for remote sensing and autonomous in situ observation, Earth-Science Reviews, 104359, https://doi.org/10.1016/j.earscirev.2023.104359, 2023.

Nowicki, M., DeVries, T., and Siegel, D. A.: Quantifying the Carbon Export and Sequestration Pathways of the Ocean’s Biological Carbon Pump, Global Biogeochemical Cycles, 36, e2021GB007083, https://doi.org/10.1029/2021GB007083, 2022.

Passow, U. and Carlson, C.: The biological pump in a high CO2 world, Mar. Ecol. Prog. Ser., 470, 249–271, https://doi.org/10.3354/meps09985, 2012.

a mis en forme : Police :Cambria Math

a mis en forme : Police :Arial

Picard, T., Gula, J., Fablet, R., Collin, J., and Mémery, L.: Predicting particle catchment areas of deep-ocean sediment traps using machine learning, Ocean Sci., 20, 1149–1165, https://doi.org/10.5194/os-20-1149-2024, 2024.

Picard, T., Baker, C. A., Gula, J., Fablet, R., Mémery, L., and Lampitt, R.: Estimating the variability of deep-ocean particle flux collected by sediment traps using satellite data and machine learning, Biogeosciences, 22, 4309–4331, https://doi.org/10.5194/bg-22-4309-2025, 2025.

Pilskaln, C. H. and Honjo, S.: The Fecal Pellet fraction of biogeochemical particle fluxes to the deep sea, Global Biogeochem. Cycles, 1, 31–48, https://doi.org/10.1029/GB001i001p00031, 1987.

Planchat, A., Kwiatkowski, L., Bopp, L., Torres, O., Christian, J. R., Butenschön, M., ... & Stock, C.: The representation of alkalinity and the carbonate pump from CMIP5 to CMIP6 Earth system models and implications for the carbon cycle. Biogeosciences, 20(7), 1195-1257. 2023

Planchat, A., Bopp, L., Kwiatkowski, L., & Torres, O. The carbonate pump feedback on alkalinity and the carbon cycle in the 21st century and beyond. Earth System Dynamics, 15(3), 565-588. 2024

Poulton, A. J., Adey, T. R., Balch, W. M., & Holligan, P. M. Relating coccolithophore calcification rates to phytoplankton community dynamics: Regional differences and implications for carbon export. Deep Sea Research Part II: Topical Studies in Oceanography, 54(5-7), 538-557. 2007.

Poulton, A. J., Stinchcombe, M. C., Achterberg, E. P., Bakker, D. C. E., Dumousseaud, C., Lawson, H. E., Lee, G. A., Richier, S., Suggett, D. J., and Young, J. R.: Coccolithophores on the north-west European shelf: calcification rates and environmental controls, Biogeosciences, 11, 3919–3940, https://doi.org/10.5194/bg-11-3919-2014, 2014.

Renforth, P., & Henderson, G.: Assessing ocean alkalinity for carbon sequestration. Reviews of Geophysics, 55(3), 636-674. 2017.

Ricour, F., Guidi, L., Gehlen, M., DeVries, T., and Legendre, L.: Century-scale carbon sequestration flux throughout the ocean by the biological pump, Nat. Geosci., 1–9, https://doi.org/10.1038/s41561-023-01318-9, 2023.

Romero, O. E., Fischer, G., Karstensen, J., and Cermeño, P.: Eddies as trigger for diatom productivity in the open-ocean Northeast Atlantic, Progress in Oceanography, 147, 38–48, https://doi.org/10.1016/j.pocean.2016.07.011, 2016.

Rosengard, S. Z., Lam, P. J., Balch, W. M., Auro, M. E., Pike, S., Drapeau, D., and Bowler, B.: Carbon export and transfer to depth across the Southern Ocean Great Calcite Belt, Biogeosciences, 12, 3953–3971, https://doi.org/10.5194/bg-12-3953-2015, 2015.

Roth, P. H., Mullin, M. M., and Berger, W. H.: Coccolith Sedimentation by Fecal Pellets: Laboratory Experiments and Field Observations, Geol Soc America Bull, 86, 1079, https://doi.org/10.1130/0016-7606(1975)86<1079:CSBFPL>2.0.CO;2, 1975.

Ryan-Keogh, T. J., Thomalla, S. J., Chang, N., & Moalusi, T. A new global oceanic multi-model net primary productivity data product. Earth System Science Data, 15(11), 4829-4848. 2023.

Samtleben, C. and Bickert, T.: Coccoliths in sediment traps from the Norwegian Sea, Marine Micropaleontology, 16, 39–64, https://doi.org/10.1016/0377-8398(90)90028-K, 1990.

Sarmiento, J. L.: Ocean Biogeochemical Dynamics, in: Ocean Biogeochemical Dynamics, Princeton University Press, https://doi.org/10.1515/9781400849079, 2013.

Savoye, N., Benitez-Nelson, C., Burd, A. B., Cochran, J. K., Charette, M., Buesseler, K. O., ... & Elskens, M.: 234Th sorption and export models in the water column: A review. Marine Chemistry, 100(3-4), 234-249. 2006.

Schiebel, R. and Movellan, A.: First-order estimate of the planktic foraminifer biomass in the modern ocean, Earth System Science Data, 4, 75–89, https://doi.org/10.5194/essd-4-75-2012, 2012.

Sulpis, O., Jeansson, E., Dinauer, A., Lauvset, S. K., and Middelburg, J. J.: Calcium carbonate dissolution patterns in the ocean, Nat. Geosci., 14, 423–428, https://doi.org/10.1038/s41561-021-00743-y, 2021.

Tamburini, C., Garel, M., Barani, A., Boeuf, D., Bonin, P., Bhairy, N., Guasco, S., Jacquet, S., Le Moigne, F. A. C., Panagiotopoulos, C., Riou, V., Veloso, S., Santinelli, C., and Armougom, F.: Increasing Hydrostatic Pressure Impacts the Prokaryotic Diversity during Emiliania huxleyi Aggregates Degradation, Water, 13, 2616, https://doi.org/10.3390/w13192616, 2021.

Thuiller, W., Pollock, L. J., Gueguen, M., and Münkemüller, T.: From species distributions to meta-communities, Ecology Letters, 18, 1321–1328, https://doi.org/10.1111/ele.12526, 2015.

Torres Valdés, S., Painter, S. C., Martin, A. P., Sanders, R., and Felden, J.: Data compilation of fluxes of sedimenting material from sediment traps in the Atlantic Ocean, Earth System Science Data, 6, 123–145, https://doi.org/10.5194/essd-6-123-2014, 2014.

Toullec, J., Vincent, D., Frohn, L., Miner, P., Le Goff, M., Devesa, J., and Moriceau, B.: Copepod Grazing Influences Diatom Aggregation and Particle Dynamics, Frontiers in Marine Science, 6, https://doi.org/10.3389/fmars.2019.00751, 2019.

Toullec, J., Delegrange, A., Perruchon, A., Duong, G., Cornille, V., Brutier, L., and Hermoso, M.: Copepod Feeding Responses to Changes in Coccolithophore Size and Carbon Content, Journal of Marine Science and Engineering, 10, 1807, https://doi.org/10.3390/jmse10121807, 2022.

Tyrrell, T. and Merico, A.: Emiliania huxleyi: bloom observations and the conditions that induce them, in: Coccolithophores: From Molecular Processes to Global Impact, edited by: Thierstein, H. R. and Young, J. R., Springer, Berlin, Heidelberg, 75–97, https://doi.org/10.1007/978-3-662-06278-4_4, 2004.

Tyrrell, T. Calcium carbonate cycling in future oceans and its influence on future climates. Journal of plankton research, 30(2), 141-156. 2008.

Vallina, S. M., Follows, M. J., Dutkiewicz, S., Montoya, J. M., Cermeno, P., and Loreau, M.: Global relationship between phytoplankton diversity and productivity in the ocean, Nat Commun, 5, 4299, https://doi.org/10.1038/ncomms5299, 2014.

Volk, T., & Hoffert, M. I. Ocean carbon pumps: Analysis of relative strengths and efficiencies in ocean-driven atmospheric CO2 changes. The carbon cycle and atmospheric CO2: Natural variations Archean to present, 32, 99-110. 1985

Wang, W.-L., Fu, W., Le Moigne, F. A. C., Letscher, R. T., Liu, Y., Tang, J.-M., and Primeau, F. W.: Biological carbon pump estimate based on multidecadal hydrographic data, Nature, 1–7, https://doi.org/10.1038/s41586-023-06772-4, 2023.

a mis en forme : Police :Cambria Math

a mis en forme : Police :Arial

a mis en forme : Police :Cambria Math

a mis en forme : Police :Arial

Wassmann, P.: Retention versus export food chains: processes controlling sinking loss from marine pelagic systems, in: Eutrophication in Planktonic Ecosystems: Food Web Dynamics and Elemental Cycling: Proceedings of the Fourth International PELAG Symposium, held in Helsinki, Finland, 26–30 August 1996, edited by: Tamminen, T. and Kuosa, H., Springer Netherlands, Dordrecht, 29–57, https://doi.org/10.1007/978-94-017-1493-8_3, 1998.

Weber, T., Cram, J. A., Leung, S. W., DeVries, T., & Deutsch, C. Deep ocean nutrients imply large latitudinal variation in particle transfer efficiency. Proceedings of the National Academy of Sciences, 113(31), 8606-8611. 2016.

Ziveri, P., Langer, G., Chaabane, S., de Vries, J., Gray, W. R., Keul, N., ... & Mortyn, P. G.: Calcifying plankton: From biomineralization to global change. Science, 390(6771), https://doi/abs/10.1126/science.adq8520. 2025~~Gray, W. R., Anglada-Ortiz, G., Manno, C., Grelaud, M., Incarbona, A., Rae, J. W. B., Subhas, A. V., Pallacks, S., White, A., Adkins, J. F., and Berelson, W.: Pelagic calcium carbonate production and shallow dissolution in the North Pacific Ocean, Nat Commun, 14, 1–14, https://doi.org/10.1038/s41467-023-36177-w, 2023~~.

Ziveri, P., Gray, W. R., Anglada-Ortiz, G., Manno, C., Grelaud, M., Incarbona, A., Rae, J. W. B., Subhas, A. V., Pallacks, S., White, A., Adkins, J. F., and Berelson, W.: Pelagic calcium carbonate production and shallow dissolution in the North Pacific Ocean, Nat Commun, 14, 1–14, https://doi.org/10.1038/s41467-023-36177-w, 2023.

Zöllner, E., Hoppe, H.-G., Sommer, U., and Jürgens, K.: Effect of zooplankton-mediated trophic cascades on marine microbial food web components (bacteria, nanoflagellates, ciliates), Limnology and Oceanography, 54, 262–275, https://doi.org/10.4319/lo.2009.54.1.0262, 2009.

a mis en forme : Police :Arial, Anglais (États-Unis)

a mis en forme : Police :Arial

a mis en forme : Police :Arial, Anglais (États-Unis)

a mis en forme : Police :Arial

a mis en forme : Police :Arial